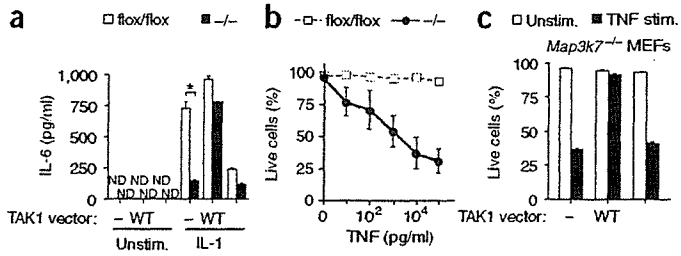

Figure 2 Impaired responses to IL-1β and TNF in *Map3k7* $^{-/-}$ MEFs. (a) IL-6 production by MEFs. Control *Map3k7*$^{flox/flox}$ and *Map3k7* $^{-/-}$ MEFs were transfected with empty ( ), wild-type TAK1 (WT) or TAK1Δ (Δ) plasmid, and then were stimulated for 24 h with 10 ng/ml of IL-1β. IL-6 in the culture medium was measured by ELISA. Data are mean ± s.d. of triplicate samples of one representative from three independent experiments. *, $P < 0.005$, versus TAK1-deficient cells (Student's *t*-test). ND, not detected. (b) Viability of control and *Map3k7* $^{-/-}$ MEFs treated for 24 h with various concentrations of TNF (horizontal axis), assessed by annexin V–indocarbocyanine staining. Three independent experiments were done in triplicate. Data are mean ± s.d. percentage of viable cells after treatment relative to untreated control. (c) Viability of control and *Map3k7* $^{-/-}$ MEFs left untransfected or transfected with wild-type or mutated TAK1 and were left unstimulated (Unstim.) or were stimulated for 24 h with 10 ng/ml of TNF (TNF stim.). Data represent mean ± s.d. for percentage of viable cells after treatment relative to untreated control.

the ability to activate NF-κB and AP-1, we did a reporter assay. Overexpression of wild-type TAK1, but not TAK1Δ, together with TAB1 in human embryonic kidney 293 (HEK293) cells activated NF-κB and AP-1, indicating that TAK1Δ was nonfunctional because it lacked an ATP-binding site (**Fig. 1f**).

TAK1 is required for IL-1β and TNF responsiveness

We first examined responses to IL-1β and TNF. We stimulated *Map3k7* $^{-/-}$ and control *Map3k7*$^{flox/flox}$ MEFs with IL-1β and measured IL-6 production by enzyme-linked immunosorbent assay (ELISA). Production of IL-6 was impaired considerably in *Map3k7* $^{-/-}$ MEFs compared with that in control cells (**Fig. 2a**). Moreover, re-expression of wild-type TAK1 but not TAK1Δ in *Map3k7* $^{-/-}$ MEFs restored IL-6 production in response to IL-1β.

As NF-κB activation is required for survival of MEFs after exposure to TNF, we next compared the viability of TNF-stimulated cells. TNF stimulation induced cell death in *Map3k7* $^{-/-}$ MEFs in a dose-dependent way (**Fig. 2b**). In contrast, *Map3k7*$^{flox/flox}$ MEFs were viable after TNF stimulation. The TNF-induced cell death noted in *Map3k7* $^{-/-}$ MEFs was circumvented by expression of wild-type TAK1 but not TAK1Δ (**Fig. 2c**). These results indicate that TAK1 is required for IL-1β- and TNF-mediated cellular responses.

We further examined the activation of signaling molecules. In both *Map3k7*$^{flox/flox}$ and *Map3k7* $^{-/-}$ MEFs, IRAK-1 was phosphorylated, ubiquitinated and degraded in response to IL-1β, indicating that TAK1 was not involved in IRAK-1 activation (**Fig. 3a**). Induction of NF-κB DNA binding and degradation of IκBα in response to IL-1β and TNF were compromised in *Map3k7* $^{-/-}$ MEFs (**Fig. 3b**). Furthermore, activation of Jnk and p38 in response to IL-1β and TNF in *Map3k7* $^{-/-}$ MEFs was also impaired (**Fig. 3c**). Thus, TAK1 was required for NF-κB, Jnk and p38 activation in response to IL-1β and TNF in MEF cells.

Generation of mice with B cell–specific TAK1 deficiency

Although the involvement of TAK1 in the IL-1β signaling has been studied extensively, its involvement in the TLR signaling pathway is less understood. Because B cells express various TLRs and respond to their ligands to proliferate, we generated mice with B cell–specific TAK1 deficiency by breeding *Map3k7*$^{flox/}$ mice with mice carrying the *Cre* transgene under control of the *Cd19* promoter (*Cd19*$^{Cre/+}$). Southern blot analysis showed almost complete Cre-mediated deletion of *Map3k7* in B cells from *Cd19*$^{Cre/+}$*Map3k7*$^{flox/}$ mice (**Supplementary Fig. 2** online). We also checked deletion of TAK1 in purified B cells by immunoblot analysis and confirmed that the expression of wild-type TAK1 was considerably reduced in B cells from *Cd19*$^{Cre/+}$*Map3k7*$^{flox/}$ mice (**Supplementary Fig. 2** online).

TAK1 deficiency impairs B-1 B cell development

We investigated whether B cell–specific TAK1 deficiency affected lymphopoiesis. The population of B cell precursors in the bone marrow was comparable in *Cd19*$^{Cre/+}$*Map3k7*$^{flox/+}$ and *Cd19*$^{Cre/+}$*Map3k7*$^{flox/}$ mice (**Fig. 4a**). The ratio of B cells to T cells, the expression of surface immunoglobulin M (IgM) and IgD on mature splenic B cells and the numbers of marginal zone B cells (IgM$^+$CD23$^-$ CD21$^+$) were also comparable for *Cd19*$^{Cre/+}$*Map3k7*$^{flox/+}$ and *Cd19*$^{Cre/+}$*Map3k7*$^{flox/}$ splenocyte samples (**Fig. 4b**). However, the B220$^+$CD5$^+$ B-1 B cell population was reduced in the peritoneal cavities of *Cd19*$^{Cre/+}$*Map3k7*$^{flox/}$ mice (**Fig. 4c**). These results indicate that TAK1 was required for the development of B-1 B cells but not of splenic follicular and marginal zone B cells.

TAK1 is required for the TLR signaling in B cells

B cells become active and progress through the cell cycle in response to TLR ligands such as LPS, CpG DNA and poly(I:C). Although *Cd19*$^{Cre/+}$*Map3k7*$^{flox/+}$ B cells proliferated in response to all TLR

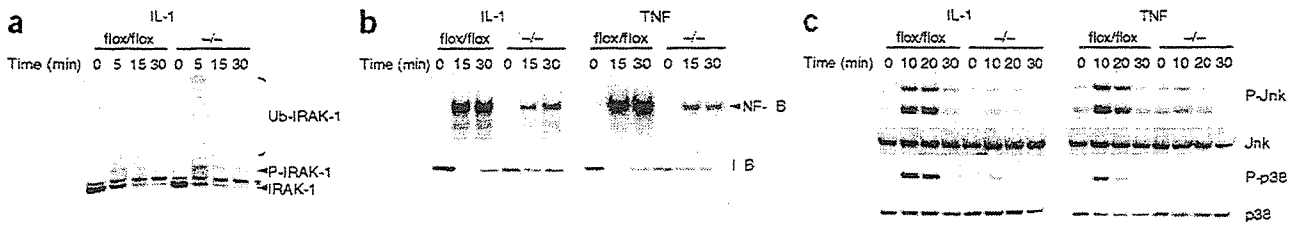

Figure 3 Impaired activation of NF-κB and MAPKs in response to IL-1β and TNF in TAK1-deficient cells. (a) Immunoblot of IRAK-1 in whole-cell lysates of control and *Map3k7* $^{-/-}$ MEFs left untreated or treated with 10 ng/ml of IL-1β (time, above lanes). Ub-, ubiquitinated; P-, phosphorylated; *, nonspecific band. (b) Control and *Map3k7* $^{-/-}$ MEFs were treated with IL-1β (10 ng/ml) or TNF (10 ng/ml) for various times (above lanes). The NF-κB DNA-binding activity in nuclear extracts was determined by EMSA (top). Degradation of IκBα whole-cell lysates was detected by immunoblot with anti-IκBα (bottom). (c) Phosphorylation of Jnk and p38 (P-Jnk and P-p38, respectively) in whole-cell lysates of control and *Map3k7* $^{-/-}$ MEFs treated with IL-1β (10 ng/ml) or TNF (10 ng/ml) for various times (above lanes), assessed by immunoblot with phosphorylation-specific antibodies. Jnk and p38, loading controls. All results are representative of three different experiments.

ligands tested, the proliferation of B cells from *Cd19*$^{Cre/+}$*Map3k7*$^{flox/}$ mice was considerably impaired (**Fig. 5a**). In addition, follicular and marginal zone B-2 cells purified from *Cd19*$^{Cre/+}$*Map3k7*$^{flox/}$ spleens had impaired proliferative responses to LPS and/or CpG DNA (**Supplementary Fig. 3** online). We also investigated cell cycle profiles by staining with bromodeoxyuridine (BrdU) and 7-amino-actinomycin D. Unlike *Cd19*$^{Cre/+}$*Map3k7*$^{flox/+}$ B cells, whose cell cycles progressed into S phase, *Cd19*$^{Cre/+}$*Map3k7*$^{flox/}$ B cells showed impaired entry to S phase after treatment with LPS and CpG DNA (**Fig. 5b**). These results indicate that TAK1 is responsible for TLR-mediated responses in B cells.

We next examined whether TAK1 deficiency influences the viability of B cells. When control B cells were cultured *ex vivo* without mitogens, 50% of the cells spontaneously underwent apoptosis within 12 h of culture (**Fig. 5c**). Stimulation with LPS or CpG DNA prevented the execution of apoptosis in control B cells. In contrast, prevention of cell death in response to LPS or CpG DNA was impaired in *Cd19*$^{Cre/+}$*Map3k7*$^{flox/}$ B cells. These results indicate that TAK1 is critical for TLR ligand–mediated prevention of B cell death.

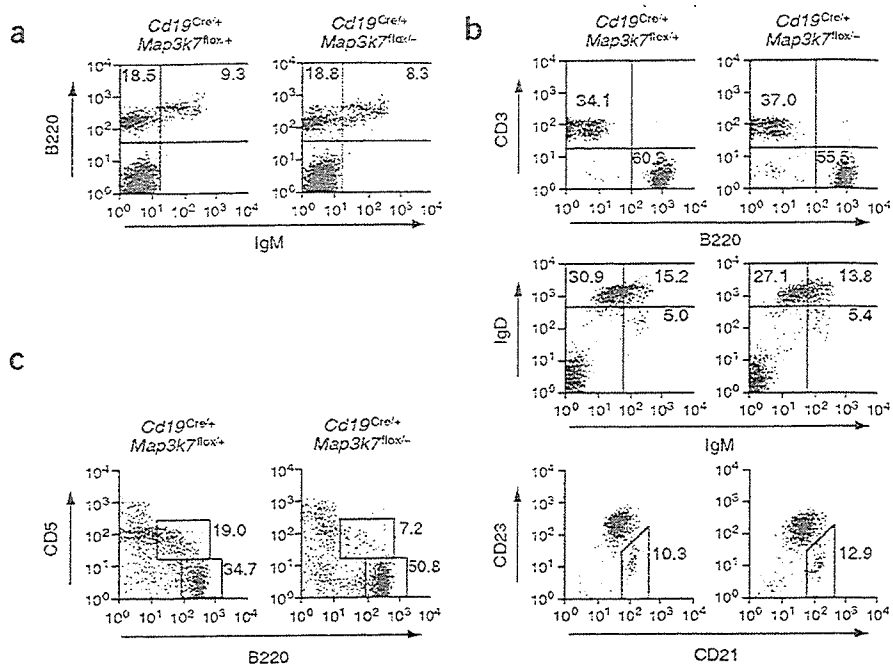

Figure 4 B cell development in *Cd19*$^{Cre/+}$*Map3k7*$^{flox/}$ mice. Flow cytometry of B cell development in the bone marrow (**a**), splenic (**b**) and peritoneal (**c**) B cells from 8-week-old *Cd19*$^{Cre/+}$*Map3k7*$^{flox/+}$ and *Cd19*$^{Cre/+}$*Map3k7*$^{flox/}$ mice. Numbers in the quadrants or beside boxed areas indicate the percentage of positive cells in that region. Results are representative of four different experiments.

We further analyzed the upregulation of surface activation markers in response to TLR stimuli. In accordance with defects in cell proliferation and apoptosis inhibition, *Cd19*$^{Cre/+}$*Map3k7*$^{flox/}$ B cells stimulated with LPS or CpG DNA showed impaired upregulation of cell surface CD69 and CD86 expression (**Fig. 5d**). It has been reported that CpG DNA induces IL-6 production from human naive B cells[20]. In mouse splenic B cells, IL-6 was produced in response to CpG DNA and LPS (**Fig. 5e**). However, IL-6 production by *Cd19*$^{Cre/+}$*Map3k7*$^{flox/}$ B cells in response to either LPS or CpG DNA was less than that of control *Cd19*$^{Cre/+}$*Map3k7*$^{flox/+}$ B cells.

We also assessed TLR-induced activation of signaling pathways in TAK1-deficient B cells. In *Cd19*$^{Cre/+}$*Map3k7*$^{flox/+}$ B cells, stimulation with LPS or CpG DNA resulted in degradation of IκBα and activation of NF-κB DNA-binding activity (**Fig. 5f,g**). In contrast, IκBα degradation and NF-κB DNA-binding activity in response to LPS and CpG DNA were reduced considerably in *Cd19*$^{Cre/+}$*Map3k7*$^{flox/}$ B cells. In addition, activation of Jnk, p38 and Erk was impaired in LPS- and CpG DNA–stimulated *Cd19*$^{Cre/+}$*Map3k7*$^{flox/}$ B cells (**Fig. 5h**). These findings indicate that TAK1 is critical for TLR-mediated B cell activation and signaling.

Requirement for TAK1 for activation of BCR signaling

BCR signaling also activates NF-κB and MAPKs, leading to B cell activation. Crosslinking of BCRs induces activation of tyrosine kinases, an increase in intracellular calcium and activation of protein kinase C-β[21]. A complex of the signaling molecules CARD11 (also known as CARMA1), Bcl10 and MALT1 (also known as paracaspase) then transduces signals to NF-κB and MAPKs downstream of protein kinase C-β[22]. It has also been proposed that TAK1 is involved in T cell receptor signaling downstream of TRAF6 to activate NF-κB[23]. However, the function of TAK1 in BCR signaling is unknown. We therefore analyzed activation of TAK1-deficient B cells in response to BCR crosslinking. Inactivation of TAK1 considerably impaired the proliferation of purified B cells in response to BCR and CD40 stimulation, similar to their response to TLR ligands, indicating that TAK1 is involved in the signaling pathways used by BCRs and CD40 (**Fig. 6a** and **Supplementary Fig. 3** online). Furthermore, *Cd19*$^{Cre/+}$*Map3k7*$^{flox/}$ B cells showed impaired entry to S phase and impaired enhancement of cell survival after BCR crosslinking compared with that of control *Cd19*$^{Cre/+}$*Map3k7*$^{flox/+}$ B cells (**Fig. 6b,c**). In contrast, BCR stimulation induced almost similar upregulation of CD69 and CD86 in control and *Cd19*$^{Cre/+}$*Map3k7*$^{flox/}$ B cells (**Fig. 6d**).

We next examined the activation of BCR-mediated signaling pathways in further detail. Tyrosine phosphorylation of cytoplasmic proteins in response to BCR stimulation was not altered in *Cd19*$^{Cre/+}$*Map3k7*$^{flox/}$ B cells (**Fig. 6e**). Unexpectedly, BCR-mediated activation of NF-κB was not impaired in TAK1-deficient B cells (**Fig. 6f,g**). Among MAPKs, activation of Jnk but not p38 or Erk was considerably impaired (**Fig. 6h**). These data demonstrate that the requirement for TAK1 in NF-κB activation differs depending on the stimuli, whereas TAK1 functions as an essential activator of Jnk in response to a variety of stimuli.

To further elucidate how TAK1 regulates BCR-mediated proliferative responses, we investigated BCR-induced gene expression profiles by microarray analysis. The BCR-mediated expression of genes involved in cell cycling and survival was not impaired in *Cd19*$^{Cre/+}$*Map3k7*$^{flox/}$ B cells (**Supplementary Table 1** online). The upregulation of cyclin D2 protein as well as mRNA was comparable in BCR-stimulated control and TAK1-deficient B cells (**Supplementary Fig. 4** and **Supplementary Table 1** online). However, the downregulation of p27^{Kip1} expression was impaired in *Cd19*$^{Cre/+}$*Map3k7*$^{flox/}$ B cells, suggesting that G1-S progression was impaired at the level of p27 expression (**Supplementary Fig. 4** online).

Bcl10 and CARD11 are crucial for BCR-induced Jnk and NF-κB activation. In contrast, MALT1 is required for the activation of NF-κB

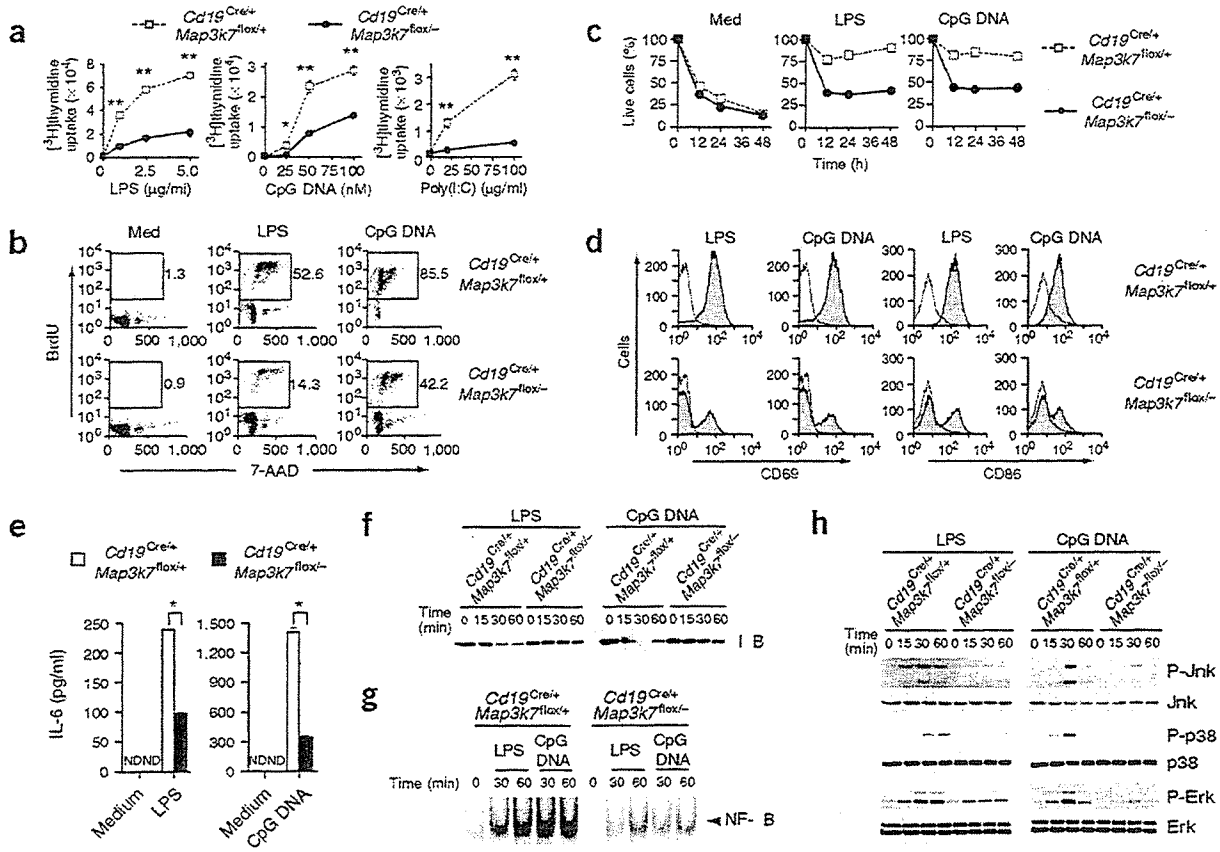

Figure 5 Impaired B cell activation in response to TLR ligands in *Cd19*$^{Cre/+}$*Map3k7*$^{flox/}$ mice. (**a**) Proliferation of purified splenic B cells treated 48 h with various stimuli (horizontal axes), assessed by [^{3}H]thymidine incorporation. Data are mean ± s.d. of triplicate cultures. *, $P < 0.05$ and **, $P < 0.005$, versus TAK1-deficient cells (Student's *t*-test). (**b**) Cell cycle profiles of B cells left untreated (Med) or after *in vitro* stimulation with 5 μg/ml of LPS or 100 nM CpG DNA. Cells were labeled with BrdU and were analyzed by flow cytometry 24 h after stimulation. Numbers beside boxed areas indicate percentage of cells in S phase. (**c**) Defective survival of *Cd19*$^{Cre/+}$*Map3k7*$^{flox/}$ cells. B cells were stimulated with 5 μg/ml of LPS or 100 nM CpG DNA. Viability of cells was assessed by staining with annexin V–indocarbocyanine followed by flow cytometry (time, horizontal axes). (**d**) Surface expression of activation markers. B cells were left unstimulated (open) or were stimulated for 24 h with 5 μg/ml of LPS or 100 nM CpG DNA (filled). Cells were then stained with anti-CD69 or anti-CD86. (**e**) ELISA of IL-6 production by B cells stimulated with LPS (20 μg/ml) or CpG DNA (2 μM). Data are mean ± s.d. of triplicate samples of one representative of three independent experiments. *, $P < 0.005$, versus TAK1-deficient cells (Student's *t*-test). (**f**) Immunoblot of IκBα degradation by B cells in response to LPS (20 μg/ml) or CpG DNA (2 μM). (**g**) EMSA of NF-κB DNA-binding activity in nuclear extracts of purified splenic B cells treated (time, above lanes) with LPS (20 μg/ml) or CpG DNA (2 μM). (**h**) Immunoblot of lysates of B cells stimulated (time, above lanes) with LPS (20 μg/ml) or CpG DNA (2 μM). Antibodies, right margin. All results are representative of three different experiments.

but not Jnk downstream of Bcl10 in BCR signaling. Mice lacking Bcl10, CARD11 or MALT1 are reported to have defects in the development of B-1 B cells and B cell activation. That prompted us to hypothesize that TAK1 may be recruited to the Bcl10 complex to activate Jnk. Therefore, we examined the association of TAK1 and Bcl10 using the human B cell line WEHI-231. When the cells were stimulated with antibody to IgM (anti-IgM), Bcl10 was immunoprecipitated together with TAK1 and with CARD11 (**Fig. 6i**). In contrast, TAK1 failed to precipitate together with Bcl10 in LPS-stimulated cells (**Fig. 6i**). These results suggest that TAK1 is recruited to the Bcl10 complex after BCR stimulation and is involved in Bcl10-mediated Jnk activation in B cells.

TAK1 is required for *in vivo* immune responses

We further investigated the involvement of TAK1 in humoral immune responses. The serum immunoglobulin concentrations of all isotypes except IgM were lower in *Cd19*$^{Cre/+}$*Map3k7*$^{flox/}$ B cells than in *Cd19*$^{Cre/+}$*Map3k7*$^{flox/+}$ B cells (**Fig. 7a**). To induce humoral immune responses, we challenged *Cd19*$^{Cre/+}$*Map3k7*$^{flox/}$ and littermate *Cd19*$^{Cre/+}$*Map3k7*$^{flox/+}$ mice with the T cell–dependent antigen nitrophenol conjugated to chicken γ-globulin or with the T cell–independent type II antigen trinitrophenol conjugated to Ficoll. The production of antigen-specific IgG1 in response to the T cell–dependent antigen was considerably impaired in *Cd19*$^{Cre/+}$*Map3k7*$^{flox/}$ mice compared with that of control *Cd19*$^{Cre/+}$*Map3k7*$^{flox/+}$ mice, whereas IgM titers were similar in both groups of mice (**Fig. 7b**). Similarly, IgG3 production of *Cd19*$^{Cre/+}$*Map3k7*$^{flox/}$ mice injected with trinitrophenol-Ficoll was impaired compared with that of control mice (**Fig. 7c**). This might have been due to the reduction in B-1 B cells in *Cd19*$^{Cre/+}$*Map3k7*$^{flox/}$ mice, as B-1 B cells are the chief mediators of the T cell–independent response[24]. Impaired activation of B cells may also contribute to the defect in the istype switching. These results show that TAK1 is required for the appropriate induction of humoral immune responses.

DISCUSSION

Here we generated TAK1-deficient mice and a mouse strain with conditional expression of a *Map3k7* allele. *In vitro* studies have

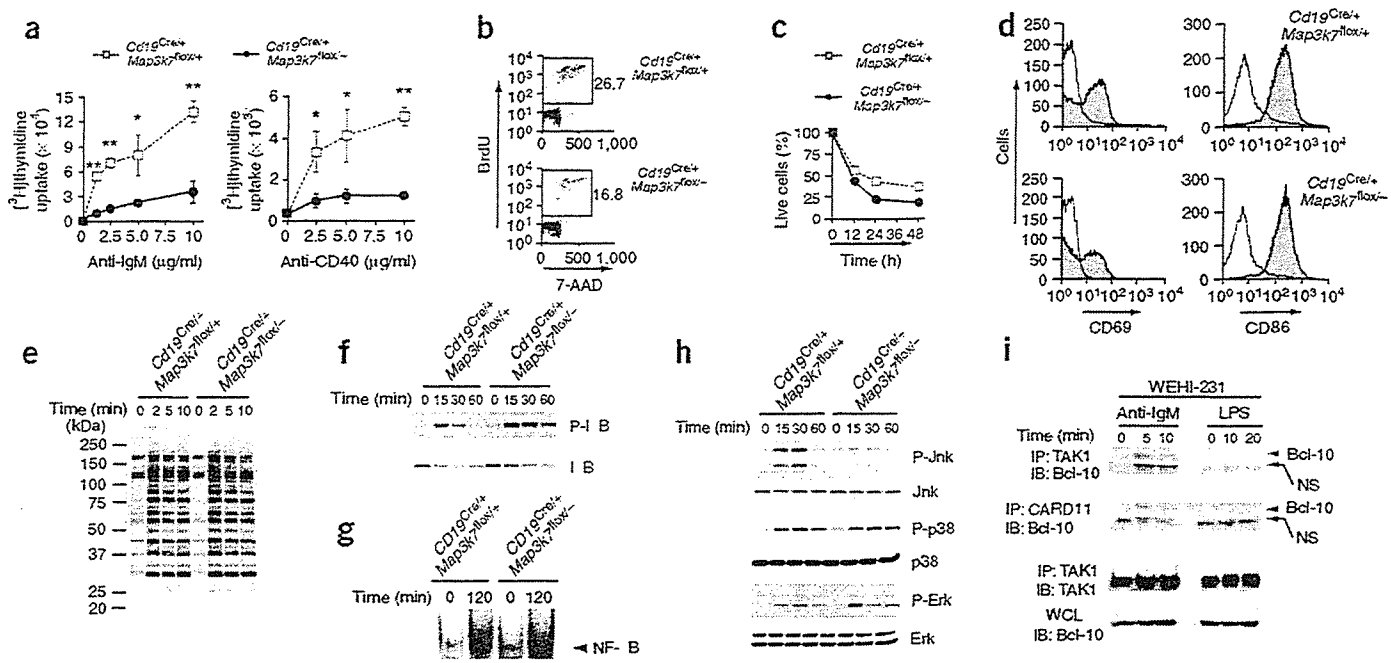

Figure 6 Impaired B cell activation by crosslinking of BCRs in *Cd19*$^{Cre/+}$*Map3k7*$^{flox/}$ mice. **(a)** Proliferation of purified splenic B cells stimulated for 48 h (stimuli, horizontal axes), assessed by [^{3}H]thymidine incorporation. Data are mean ± s.d. of triplicate cultures. *, $P < 0.05$ and **, $P < 0.005$, versus TAK1-deficient cells (Student's *t*-test). **(b)** Cell cycle profiles of B cells stimulated with 5 μg/ml of anti-IgM. Cells were labeled with BrdU and were analyzed by flow cytometry 24 h after stimulation. Numbers beside boxed areas indicate percentages of cells in S phase. **(c)** Viability of B cells stimulated with 5 μg/ml of anti-IgM, assessed by staining with annexin V–indocarbocyanine followed by flow cytometry (time, horizontal axis). **(d)** Flow cytometry of purified splenic B cells left unstimulated (open) or stimulated for 24 h with 5 μg/ml of anti-IgM (filled) and then stained with anti-CD69 or anti-CD86. **(e)** Total tyrosine phosphorylation of B cells stimulated with 20 μg/ml of anti-IgM (time, above lanes). **(f)** Immunoblot of IκBα degradation in B cells in response to 20 μg/ml of anti-IgM. **(g)** EMSA of NF-κB DNA-binding activity in nuclear extracts from purified splenic B cells stimulated for 2 h with 20 μg/ml of anti-IgM. **(h)** MAPK activation in BCR-stimulated B cells stimulated with 20 μg/ml of anti-IgM (time, above lanes). **(i)** Association between TAK1 and Bcl10. WEHI-231 cells (1.5 10^8) were stimulated with 20 μg/ml of anti-IgM or 20 μg/ml of LPS (time, above lanes); cell lysates were immunoprecipitated (IP) with anti-TAK1 or anti-CARD11 and immunoprecipitates or whole-cell lysates (WCL) were analyzed by immunoblot (IB; antibodies, left margin). All results are representative of three different experiments. NS, nonspecific band.

suggested that TAK1 has an important function in IL-1R and TNFR signaling by forming a complex with TAB1 and TAB2 (refs. 11,14,15). However, mice lacking TAB2 have normal IL-1β responses[18]. The function of TAB1 in the IL-1R signaling is still unclear, although involvement TAB1 in TGF-β signaling has been reported in studies of TAB1-deficient mice[19]. It is possible TAB3, a homolog of TAB2, functions redundantly in TAB2-deficient mice[16,17,25,26]. In contrast, TAK1-deficient MEFs showed considerably impaired responses, including activation of NF-κB and MAPKs in response to IL-1β stimulation. However, IL-1β-induced production of IL-6 or activation of NF-κB was not completely abrogated in TAK1-deficient MEFs, indicating IL-1R activates both TAK1-dependent and TAK1-independent signaling pathways.

The involvement of TAK1 in TNFR signaling is controversial. Initially, TAK1 was reported to bind TRAF6 but not TRAF2, an important mediator of TNFR signaling[8]. However, other *in vitro* studies have shown that TAK1 regulates TNF-induced NF-κB activation[11,26]. Our results have demonstrated that TAK1 is critical for activation of both NF-κB and MAPKs in response to TNF. In addition, stimulation with TNF alone induced massive cell death in *Map3k7* $^{/}$ MEFs. In wild-type cells, TNF stimulation activates NF-κB and MAPK pathways, which mediate cell survival and proliferation by expressing target genes such as those encoding inhibitor of apoptosis and Bcl-2 family members[1]. TNF simultaneously activates the apoptotic pathway by recruiting Fas-associated death domain and caspase 8, followed by activation of caspase 3. This pathway does not require protein synthesis[1]. It is believed that the balance between life and death signals determines the fate of the cell. TNF kills wild-type cells when protein synthesis is inhibited. Given that TNF-induced NF-κB and MAPK activation was considerably impaired in *Map3k7* $^{/}$ MEFs, cells lacking TAK1 might fail to induce survival genes that protect cells from TNF-induced cell death.

The function of TAK1 in TLR signaling is less well understood. As B cells express various TLRs and are activated in response to pathogen-associated molecular patterns, we examined the involvement of TAK1 in TLR signaling using the B cell system as a model. Although most TLRs as well as IL-1R share MyD88 as an adaptor for triggering intracellular signaling, several other adaptor molecules such as TRIF contribute to the TLR signaling pathways[3]. Responses to TLR3, TLR4 and TLR9 ligands were considerably impaired in TAK1-defeicient B cells. Moreover, activation of MAPKs and NF-κB in response to TLR4 and TLR9 ligand was consistently impaired, although the activation was not completely abrogated even in the absence of TAK1. As TLR9 signaling depends completely on MyD88, it is obvious that TAK1 is important for MyD88-dependent signaling pathways. TLR4 activates MyD88-dependent and TRIF-dependent pathways. Both signaling pathways can activate NF-κB and MAPKs, although the time course differs. The MyD88-dependent pathway governs early activation of these signaling molecules, whereas the TRIF-dependent pathway is responsible for sustaining the activation[27,28]. In B cells, both MyD88 and TRIF are required for TLR4-induced proliferative response. In TLR4 signaling, the activation of NF-κB and MAPKs was considerably

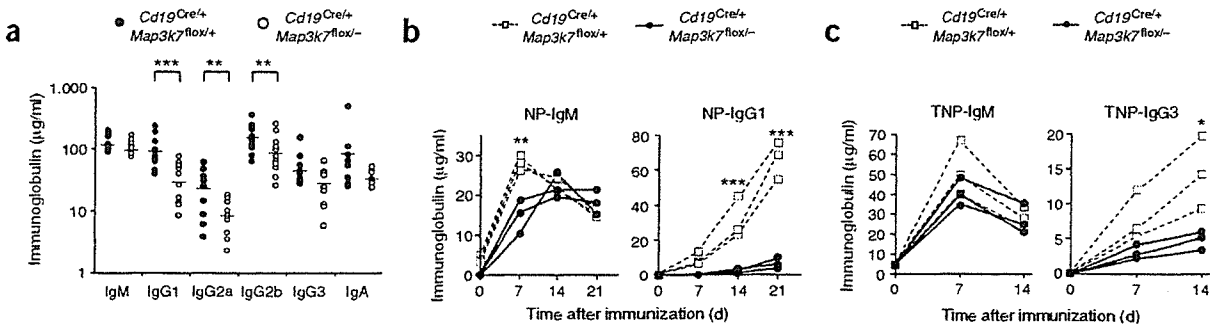

Figure 7 Impaired immune responses in *Cd19*$^{Cre/+}$*Map3k7*$^{flox/}$ mice. (**a**) Reduced basal immunoglobulin titers in *Cd19*$^{Cre/+}$*Map3k7*$^{flox/}$ mice. Immunoglobulin isotypes were measured by ELISA in the sera of nonimmunized 8-week-old *Cd19*$^{Cre/+}$*Map3k7*$^{flox/+}$ mice ($n = 12$) or *Cd19*$^{Cre/+}$*Map3k7*$^{flox/}$ mice ($n = 12$). Results are from individual mice. (**b**) Impaired T cell–dependent antibody responses in *Cd19*$^{Cre/+}$*Map3k7*$^{flox/}$ mice. Mice were immunized with nitrophenol–chicken γ-globulin, and nitrophenol (NP)–specific IgM and IgG1 production was measured by ELISA 7, 14 and 21 d after immunization. Results are from three (of five) representative mice per genotype. (**c**) Impaired T cell–independent type II antibody responses in *Cd19*$^{Cre/+}$*Map3k7*$^{flox/}$ mice. Mice were immunized with trinitrophenol-Ficoll, and trinitrophenol (TNP)–specific IgM and IgG3 production was measured 7 and 14 d after immunization. Results are from three (of five) representative mice per genotype. *, $P < 0.05$; **, $P < 0.01$ and ***, $P < 0.005$, versus TAK1-deficient cells (Student's *t*-test).

impaired in TAK1-deficient B cells at all time points examined, suggesting that MyD88-dependent and TRIF-dependent activation of these molecules depends entirely on TAK1.

Notably, TAK1 is also critical for B cell proliferation as well as Jnk activation in response to BCR crosslinking. Nevertheless, the activation of NF-κB and induction of NF-κB target genes induced by BCR-crosslinking was not impaired in TAK1-deficient B cells. In BCR signaling, a complex of CARD11, Bcl10 and MALT1 transduces signals to NF-κB and MAPKs downstream of protein kinase C-β[22]. CARD11 recruits Bcl10 to lipid rafts after stimulation. Bcl10 targets NF-κB essential modulator for K63-linked polyubiquitination through Ubc13 and MALT1 and activates NF-κB[29]. B cells from *Card11*$^{-/-}$, *Bcl10*$^{-/-}$ or *Malt1*$^{-/-}$ mice are reported to have defects in BCR signaling[30–36]. CARD11 is required for the activation of both NF-κB and Jnk[32]. Furthermore, *Bcl10*$^{-/-}$ B cells fail to activate NF-κB in response to BCR crosslinking. In contrast, B cells deficient in MALT1 (paracaspase) show impaired activation of NF-κB but not Jnk[34], indicating that Jnk is activated in a CARD11- and Bcl10-dependent, MALT1-independent signaling pathway. Given that TAK1 phosphorylates IKKs and MKK6 in IL-1β signaling, it is plausible that TAK1 is activated downstream of the CARD11-Bcl10-MALT1 complex and phosphorylates MAPKKs. In fact, we found that TAK1 interacted with Bcl10 in response to BCR crosslinking, indicating that TAK1 is recruited to the Bcl10 complex after BCR stimulation to induce Jnk activation. Although published work has shown that RNA interference–mediated knockdown of TAK1 in Jurkat cells results in diminished NF-κB activation in TCR signaling[23], our study has demonstrated that TAK1 is dispensable for NF-κB activation, at least in BCR signaling. That earlier report also showed that TRAF6 functions downstream of Bcl10 and MALT1 to activate NF-κB in TCR signaling[23]. Given that TAK1 interacts with Bcl10 in response to BCR but not LPS stimulation, it is likely that TAK1 is activated by Bcl10 without the intervention of TRAF6 in BCR signaling. As TAK1 is required for the activation of Jnk but not NF-κB, MALT1-mediated activation of the IKK complex probably occurs independently of TAK1. These results collectively indicate that in B cells, CARD11 and Bcl10 might activate TAK1 and MALT1 to regulate MAPKKs and IKKs, respectively.

Although TAK1-deficient B cells failed to proliferate in response to BCR crosslinking, activation of NF-κB was not impaired. Consistent with that finding, the upregulation of cyclin D2 was not altered in TAK1-deficient B cells. However, downregulation of $p27^{Kip1}$ was impaired in TAK1-deficient B cells, suggesting that TAK1-dependent signaling might regulate G1-S progression at the level of $p27^{Kip1}$ degradation. So far, it is not clear whether Jnk alone is responsible for the defect in the proliferation in TAK1-deficient B cells. It is possible that TAK1 regulates the activation of as-yet-unknown signaling pathway(s) in addition to Jnk and that the pathways cooperatively control BCR-mediated proliferation. Additional studies are needed to clarify the molecular mechanisms of cell cycle progression in BCR signaling.

Involvement of TAK1 in early embryogenesis modifying bone morphogenic protein signaling has been suggested[37]. *Map3k7*$^{-/-}$ embryos died at E9.5–E10.5. Mice deficient in genes encoding molecules involved in NF-κB signaling, such as RelA (also called p65) and IKKβ, die *in utero* due to massive liver apoptosis[38–41]. However, *Map3k7*$^{-/-}$ mice die before the initiation of fetal liver development, suggesting that the function of TAK1 in embryonic development is not explained by NF-κB inhibition. TAB1-deficient mice die between E15.5 and E18.5 due to edema and hemorrhage, and TAB2-deficient mice die between E11.5 and E12.5 due to liver apoptosis[18,19]. Thus, the function of TAK1 in embryogenesis might be independent of TAB1 or TAB2. The TAK1-NLK-STAT3 cascade is essential for TGF-β-mediated mesoderm formation in xenopus embryos[42]. Additional studies will be needed to clarify the mechanisms of the involvement of TAK1 in early embryogenesis.

In conclusion, we have shown here that TAK1 is essential for MAPK and NF-κB activation in response to TLR, IL-1R and TNFR stimulation. Consistent with those findings, TAK1-deficient cells failed to activate in response to TLR ligands, IL-1β and TNF. Antigen-induced B cell proliferation as well as immune responses to experimental antigens were considerably impaired in mice with B cell–specific TAK1-deficiency, indicating that TAK1 is involved in both innate and adaptive immunity. These data provide genetic evidence that TAK1 kinase has nonredundant functions in signaling pathways in inflammatory and immune responses.

METHODS

Generation of *Map3k7* mutant mice. Phage clones containing mouse *Map3k7* were isolated by screening of a 129/SvJ genomic library (Stratagene) with a probe corresponding to the 5′ end of mouse TAK1 cDNA. A targeting vector was designed to flank exon 2, containing the sequence encoding the ATP-binding site, with two *lox*P sites. The floxed neomycin-resistance gene fragment was inserted into intron 1 of *Map3k7*. A 1.0-kilobase (kb) *Cla*I–*Bam*HI

fragment was used as the 5′ homology region; a 2.5-kb *Xba*I–*Sal*I fragment, which contains exon 2 of *Map3k7*, was inserted between the two *lox*P sites; and a 6.0-kb *Not*I–*Sac*II fragment was used as the 3′ homology region. The herpes simplex virus thymidine kinase gene was used for negative selection of clones with random integration. A total of 30 μg of *Sac*II-linearized vector was electroporated into E14.1 embryonic stem cells. After positive and negative selection with G418 and ganciclovir, drug-resistant clones were picked up and were screened by PCR and Southern blot analysis. These clones were individually microinjected into blastocysts derived from C57BL/6 mice and were transferred to pseudopregnant females. Matings of chimeric male mice to C57BL/6 female mice resulted in transmission of the floxed allele to the germline. *Map3k7*$^{flox/+}$ or *Map3k7*$^{flox/flox}$ mice were bred with transgenic mouse line carrying the *Cre* transgene under control of the cytomegalovirus immediate early enhancer–chicken β-actin hybrid (*CAG*) promoter[43] to generate the *CAG*$^{Cre/+}$*Map3k7*$^{flox/+}$ (genotype, *Map3k7*$^{+/}$), which were then intercrossed to generate *CAG*$^{Cre/+}$*Map3k7*$^{flox/flox}$ (genotype, *Map3k7* $^{/}$) mice. All animal experiments were done with the approval of the Animal Research Committee of the Research Institute for Microbial Diseases (Osaka University, Osaka, Japan).

Establishment of *Map3k7* $^{/}$ MEFs. MEFs were obtained from E13.5 *Map3k7*$^{flox/flox}$ embryos, were immortalized according to a general 3T3 protocol[44] and were cloned. For excision of the floxed genomic fragment containing exon 2, two different clones of *Map3k7*$^{flox/flox}$ MEFs were infected with retrovirus expressing Cre protein together with GFP or were infected with GFP alone (to establish control MEFs). GFP^{+} cells were sorted by FACSVantage (Becton Dickinson) and then were analyzed by Southern blot and immunoblot to confirm genotype.

Generation of mice with B cell–specific TAK1 deficiency. Mice carrying the *Cre* transgene under control of the *Cd19* promoter[45] were bred with *Map3k7*$^{+/}$ mice to generate *Cd19*$^{Cre/+}$*Map3k7*$^{+/}$ mice. These mice were mated with *Map3k7*$^{flox/flox}$ mice; *Cd19*$^{Cre/+}$*Map3k7*$^{flox/+}$ or *Cd19*$^{Cre/+}$*Map3k7*$^{flox/}$ offspring were used for analysis.

Purification of B cells. Resting B cells were isolated from single-cell suspensions of spleen cells by depletion of CD43^{+} cells with anti-CD43 magnetic beads (MACS; Miltenyi Biotec). Cell purity was typically more than 95% B220^{+}, as assessed by flow cytometry.

Immunoblot analysis. Cells were lysed in a lysis buffer containing 1.0% Nonidet-P40, 150 mM NaCl, 20 mM Tris-HCl, pH 7.5, 1 mM EDTA and a protease inhibitor 'cocktail' (Roche). Lysates were separated by SDS-PAGE and were transferred onto polyvinylidene difluoride membranes (BioRad). After membranes were blotted with antibodies, proteins on membranes were visualized with an enhanced chemiluminescence system (Perkin-Elmer). Polyclonal anti-TAK1, anti-TAB1, anti-TAB2 and anti-IRAK-1 were as described[8,15,46]. Polyclonal antibody to phosphorylated Jnk (anti-phospho-Jnk), anti-phospho-p38, anti-phospho-Erk and anti-phospho-IκBα were purchased from Cell Signaling. Polyclonal anti-Jnk, anti-p38, anti-Erk, anti-IκBα, anti-p27^{Kip1} and anti–cyclin D2 and monoclonal anti-Bcl10 (clone 331.3) were from Santa Cruz. Monoclonal anti-phosphotyrosine (clone 4G10) was purchased from Upstate Biotechnology. Polyclonal anti-CARD11 was from Alexis Biochemicals.

Luciferase reporter assay. HEK293 cells were transiently transfected with 100 ng of either NF-κB (5) or AP-1 luciferase reporter plasmids, together with a total of 1.0 μg expression vector(s). Then, 48 h later, the luciferase activity in the total cell lysate was measured with the Dual-luciferase reporter assay system (Promega).

Measurement of IL-6 production. MEFs (2 10^{4}) and purified splenic B cells (5 10^{4}) were stimulated for 48 h with recombinant mouse IL-1β (R&D Systems) and LPS (Sigma) or with CpG DNA (ODN1668; Hokkaido System Science), respectively. Culture supernatants were collected and IL-6 was measured with an ELISA kit (R&D Systems).

Cell viability. MEFs (2 10^{5}) were seeded onto six-well plates and were treated for 24 h with various concentrations of recombinant mouse TNF (R&D Systems). Purified splenic B cells (1 10^{6}) were stimulated with LPS, CpG DNA or anti-IgM (Jackson ImmunoResearch) for various periods. Cell viability was assessed with annexin V–indocarbocyanine (BioVision) and a FACSCalibur (Becton Dickinson).

Electrophoretic mobility-shift assay (EMSA). MEFs (1 10^{6}) or purified splenic B cells (5 10^{6}) were treated with stimuli for various periods. Nuclear extracts were purified from cells, were incubated with a probe specific for the NF-κB DNA-binding site, were separated by electrophoresis and were visualized by autoradiography as described[47].

Flow cytometry. Single-cell suspensions were prepared from thymi, bone marrow, spleens and peritoneal cavities of untreated mice. Cells were stained with fluorescein isothiocyanate–, phycoerythrin- or allophycocyanin-conjugated antibodies (Pharmingen) and then were analyzed on a FACSCalibur.

***In vivo* immunization and ELISA.** Mice were immunized intraperitoneally with 50 μg nitrophenol–chicken γ-globulin (Biosearch Technologies) precipitated with Imject alum (Pierce) or with 25 μg trinitrophenol-Ficoll (Biosearch Technologies). Antigen- and isotype-specific antibodies were measured by ELISA in sera collected from peripheral blood at various time points, on plates coated with nitrophenol-BSA or trinitrophenol-BSA. Antibodies to mouse IgM, IgG1, IgG2a, IgG2b, IgG3 and IgA were purchased from Southern Biotechnology.

B cell proliferation assay. Purified splenic B cells (5 10^{4}) were cultured in 96-well plates for 48 h with various concentrations of LPS, CpG DNA, poly(I:C) (Amersham), anti-IgM or anti-CD40 (Pharmingen). Samples were pulsed with 1 μCi [^{3}H]thymidine for the last 12 h and then ^{3}H uptake was measured with a β-scintillation counter (Packard).

Cell cycle analysis. Cell cycles of B cells were analyzed with the BrdU Flow Kit (Pharmingen) according to the manufacturer's instructions. Cells were cultured with LPS, CpG DNA or anti-IgM for 24 h, were pulsed with 10 μM BrdU for an additional 16 h, were stained with fluorescein isothiocyanate–anti-BrdU and 7-amino-actinomycin D and then were analyzed by flow cytometry.

Microarray analysis. Purified splenic B cells were treated for 4 h with or without anti-IgM (20 μg/ml). Total RNA was extracted with an RNeasy kit (Qiagen), and double-stranded DNA was synthesized from 10 μg of total RNA with the SuperScript Choice System (Invitrogen) primed with a T7-Oligo primer (Affymetrix). This cDNA was used to prepare biotin-labeled cRNA by an *in vitro* transcription reaction done with T7 RNA polymerase in the presence of biotinylated ribonucleotides, according to the manufacturer's protocol (Enzo Diagnostics). The cRNA product was purified with an RNeasy kit and fragmented and was hybridized to Affymetrix mouse expression array A430.2 microarray chips according to the manufacturer's protocol (Affymetrix). The hybridized chips were stained and washed and were scanned with a GeneArray Scanner (Affymetrix).

Accession code. GEO: microarray data, GSE3065.

Note: Supplementary information is available on the Nature Immunology website.

ACKNOWLEDGMENTS

We thank R.C. Rickert (The Burnham Institute, La Jolla, California) for providing *Cd19-Cre* mice; J. Miyazaki (Osaka University, Suita, Japan) for providing *CAG-Cre* mice; T. Kitamura (University of Tokyo, Tokyo, Japan) for providing retrovirus vector; D.T. Golenbock (University of Massachusetts Medical School, Worcester, Massachusetts) for providing NF-κB reporter; T. Kaisho and Y. Kumagai for discussions; K. Nakamura for cell sorting; A. Shibano, M. Shiokawa, Y. Fujiwara and N. Kitagaki for technical assistance; and M. Hashimoto and E. Horita for secretarial assistance. Supported by Special Coordination Funds, the Ministry of Education, Culture, Sports, Science and Technology.

COMPETING INTERESTS STATEMENT

The authors declare that they have no competing financial interests.

Published online at http://www.nature.com/natureimmunology/
Reprints and permissions information is available online at http://npg.nature.com/reprintsandpermissions/

1. Aggarwal, B.B. Signalling pathways of the TNF superfamily: a double-edged sword. *Nat. Rev. Immunol.* 3, 745–756 (2003).

2. Dinarello, C.A. Biologic basis for interleukin-1 in disease. *Blood* **87**, 2095–2147 (1996).
3. Akira, S. & Takeda, K. Toll-like receptor signalling. *Nat. Rev. Immunol.* **4**, 499–511 (2004).
4. Baud, V. & Karin, M. Signal transduction by tumor necrosis factor and its relatives. *Trends Cell Biol.* **11**, 372–377 (2001).
5. Deng, L. *et al.* Activation of the IκB kinase complex by TRAF6 requires a dimeric ubiquitin-conjugating enzyme complex and a unique polyubiquitin chain. *Cell* **103**, 351–361 (2000).
6. Wang, C. *et al.* TAK1 is a ubiquitin-dependent kinase of MKK and IKK. *Nature* **412**, 346–351 (2001).
7. Ghosh, S. & Karin, M. Missing pieces in the NF-κB puzzle. *Cell* **109**, S81–S96 (2002).
8. Ninomiya-Tsuji, J. *et al.* The kinase TAK1 can activate the NIK-IκB as well as the MAP kinase cascade in the IL-1 signalling pathway. *Nature* **398**, 252–256 (1999).
9. Yamaguchi, K. *et al.* Identification of a member of the MAPKKK family as a potential mediator of TGF-β signal transduction. *Science* **270**, 2008–2011 (1995).
10. Vidal, S. *et al.* Mutations in the *Drosophila* dTAK1 gene reveal a conserved function for MAPKKKs in the control of rel/NF-κB-dependent innate immune responses. *Genes Dev.* **15**, 1900–1912 (2001).
11. Takaesu, G. *et al.* TAK1 is critical for IκB kinase-mediated activation of the NF-κB pathway. *J. Mol. Biol.* **326**, 105–115 (2003).
12. Irie, T., Muta, T. & Takeshige, K. TAK1 mediates an activation signal from toll-like receptor(s) to nuclear factor-κB in lipopolysaccharide-stimulated macrophages. *FEBS Lett.* **467**, 160–164 (2000).
13. Wan, J. *et al.* Elucidation of the c-Jun N-terminal kinase pathway mediated by Estein-Barr virus-encoded latent membrane protein 1. *Mol. Cell. Biol.* **24**, 192–199 (2004).
14. Shibuya, H. *et al.* TAB1: an activator of the TAK1 MAPKKK in TGF-β signal transduction. *Science* **272**, 1179–1182 (1996).
15. Takaesu, G. *et al.* TAB2, a novel adaptor protein, mediates activation of TAK1 MAPKKK by linking TAK1 to TRAF6 in the IL-1 signal transduction pathway. *Mol. Cell* **5**, 649–658 (2000).
16. Ishitani, T. *et al.* Role of the TAB2-related protein TAB3 in IL-1 and TNF signaling. *EMBO J.* **22**, 6277–6288 (2003).
17. Cheung, P.C., Nebreda, A.R. & Cohen, P. TAB3, a new binding partner of the protein kinase TAK1. *Biochem. J.* **378**, 27–34 (2004).
18. Sanjo, H. *et al.* TAB2 is essential for prevention of apoptosis in fetal liver but not for interleukin-1 signaling. *Mol. Cell. Biol.* **23**, 1231–1238 (2003).
19. Komatsu, Y. *et al.* Targeted disruption of the Tab1 gene causes embryonic lethality and defects in cardiovascular and lung morphogenesis. *Mech. Dev.* **119**, 239–249 (2002).
20. Wagner, M. *et al.* IL-12p70-dependent Th1 induction by human B cells requires combined activation with CD40 ligand and CpG DNA. *J. Immunol.* **172**, 954–963 (2004).
21. Kurosaki, T. Regulation of B-cell signal transduction by adaptor proteins. *Nat. Rev. Immunol.* **2**, 354–363 (2002).
22. Thome, M. CARMA1, BCL-10 and MALT1 in lymphocyte development and activation. *Nat. Rev. Immunol.* **4**, 348–359 (2004).
23. Sun, L., Deng, L., Ea, C.K., Xia, Z.P. & Chen, Z.J. The TRAF6 ubiquitin ligase and TAK1 kinase mediate IKK activation by BCL10 and MALT1 in T lymphocytes. *Mol. Cell* **14**, 289–301 (2004).
24. Sidorova, E.V., Li-Sheng, L., Devlin, B., Chernishova, I. & Gavrilova, M. Role of different B-cell subsets in the specific and polyclonal immune response to T-independent antigens type 2. *Immunol. Lett.* **88**, 37–42 (2003).
25. Jin, G. *et al.* Identification of a human NF-κB-activating protein, TAB3. *Proc. Natl. Acad. Sci. USA* **101**, 2028–2033 (2004).
26. Kanayama, A. *et al.* TAB2 and TAB3 activate the NF-κB pathway through binding to polyubiquitin chains. *Mol. Cell* **15**, 535–548 (2004).
27. Kawai, T., Adachi, O., Ogawa, T., Takeda, K. & Akira, S. Unresponsiveness of MyD88-deficient mice to endotoxin. *Immunity* **11**, 115–122 (1999).
28. Yamamoto, M. *et al.* Role of adaptor TRIF in the MyD88-independent toll-like receptor signaling pathway. *Science* **301**, 640–643 (2003).
29. Zhou, H. *et al.* Bcl10 activates the NF-κB pathway through ubiquitination of NEMO. *Nature* **427**, 167–171 (2004).
30. Ruland, J. *et al.* Bcl10 is a positive regulator of antigen receptor-induced activation of NF-κB and neural tube closure. *Cell* **104**, 33–42 (2001).
31. Egawa, T. *et al.* Requirement for CARMA1 in antigen receptor-induced NF-κB activation and lymphocyte proliferation. *Curr. Biol.* **13**, 1252–1258 (2003).
32. Hara, H. *et al.* The MAGUK family protein CARD11 is essential for lymphocyte activation. *Immunity* **18**, 763–775 (2003).
33. Newton, K. & Dixit, V.M. Mice lacking the CARD of CARMA1 exhibit defective B lymphocyte development and impaired proliferation of their B and T lymphocytes. *Curr. Biol.* **13**, 1247–1251 (2003).
34. Ruefli-Brasse, A.A., French, D.M. & Dixit, V.M. Regulation of NF-κB-dependent lymphocyte activation and development by paracaspase. *Science* **302**, 1581–1584 (2003).
35. Ruland, J., Duncan, G.S., Wakeham, A. & Mak, T.W. Differential requirement for Malt1 in T and B cell antigen receptor signaling. *Immunity* **19**, 749–758 (2003).
36. Xue, L. *et al.* Defective development and function of Bcl10-deficient follicular, marginal zone and B1 B cells. *Nat. Immunol.* **4**, 857–865 (2003).
37. Munoz-Sanjuan, I., Bell, E., Altmann, C.R., Vonica, A. & Brivanlou, A.H. Gene profiling during neural induction in *Xenopus laevis*: regulation of BMP signaling by post-transcriptional mechanisms and TAB3, a novel TAK1-binding protein. *Development* **129**, 5529–5540 (2002).
38. Beg, A.A., Sha, W.C., Bronson, R.T., Ghosh, S. & Baltimore, D. Embryonic lethality and liver degeneration in mice lacking the RelA component of NF-κB. *Nature* **376**, 167–170 (1995).
39. Tanaka, M. *et al.* Embryonic lethality, liver degeneration, and impaired NF-κB activation in IKK-β-deficient mice. *Immunity* **10**, 421–429 (1999).
40. Li, Q., Van Antwerp, D., Mercurio, F., Lee, K.F. & Verma, I.M. Severe liver degeneration in mice lacking the IκB kinase 2 gene. *Science* **284**, 321–325 (1999).
41. Rudolph, D. *et al.* Severe liver degeneration and lack of NF-κB activation in NEMO/IKKγ-deficient mice. *Genes Dev.* **14**, 854–862 (2000).
42. Ohkawara, B. *et al.* Role of the TAK1-NLK-STAT3 pathway in TGF-β-mediated mesoderm induction. *Genes Dev.* **18**, 381–386 (2004).
43. Sakai, K., Mitani, K. & Miyazaki, J. Efficient regulation of gene expression by adenovirus vector-mediated delivery of the CRE recombinase. *Biochem. Biophys. Res. Commun.* **217**, 393–401 (1995).
44. Todaro, G.J. & Green, H. Quantitative studies of the growth of mouse embryo cells in culture and their development into established lines. *J. Cell Biol.* **17**, 299–313 (1963).
45. Rickert, R.C., Roes, J. & Rajewsky, K. B lymphocyte-specific, Cre-mediated mutagenesis in mice. *Nucleic Acids Res.* **25**, 1317–1318 (1997).
46. Sato, S. *et al.* A variety of microbial components induce tolerance to lipopolysaccharide by differentially affecting MyD88-dependent and -independent pathways. *Int. Immunol.* **14**, 783–791 (2002).
47. Sato, S. *et al.* Synergy and cross-tolerance between toll-like receptor (TLR) 2- and TLR4-mediated signaling pathways. *J. Immunol.* **165**, 7096–7101 (2000).

Immunity 24, 41–51, January 2006 ©2006 Elsevier Inc. DOI 10.1016/j.immuni.2005.11.004

IκBNS Inhibits Induction of a Subset of Toll-like Receptor-Dependent Genes and Limits Inflammation

Hirotaka Kuwata,[1] Makoto Matsumoto,[1] Koji Atarashi,[1] Hideaki Morishita,[1] Tomohiro Hirotani,[2] Ritsuko Koga,[1] and Kiyoshi Takeda[1,*]
[1] Department of Molecular Genetics
Medical Institute of Bioregulation
Kyushu University
3-1-1 Maidashi, Higashi-ku
Fukuoka 812-8582
Japan
[2] Department of Gastroenterology and Hepatology
Graduate School of Medicine
Osaka University
2-2 Yamada-oka, Suita
Osaka 565-0871
Japan

Summary

Toll-like receptor (TLR)-mediated immune responses are downregulated by several mechanisms that affect signaling pathways. However, it remains elusive how TLR-mediated gene expression is differentially modulated. Here, we show that IκBNS, a TLR-inducible nuclear IκB protein, negatively regulates induction of a subset of TLR-dependent genes through inhibition of NF-κB activity. IκBNS-deficient macrophages and dendritic cells show increased TLR-mediated expression of genes such as IL-6 and IL-12p40, which are induced late after TLR stimulation. In contrast, IκBNS-deficient cells showed normal induction of genes that are induced early or induced via IRF-3 activation. LPS stimulation of IκBNS-deficient macrophages prolonged NF-κB activity at the specific promoters, indicating that IκBNS mediates termination of NF-κB activity at selective gene promoters. Moreover, IκBNS-deficient mice are highly susceptible to LPS-induced endotoxin shock and intestinal inflammation. Thus, IκBNS regulates inflammatory responses by inhibiting the induction of a subset of TLR-dependent genes through modulation of NF-κB activity.

Introduction

Toll-like receptors (TLRs) are implicated in the recognition of specific patterns of microbial components and subsequent induction of gene expression. TLR-dependent gene expression is induced through activation of two distinct signaling pathways mediated by the Toll/IL-1 receptor (TIR) domain-containing adaptors MyD88 and TRIF. These signaling pathways finally culminate in the activation of several transcription factors, such as NF-κB and IRF families (Akira and Takeda, 2004). The MyD88-dependent gene induction is achieved by an early phase of NF-κB and IRF-5 activation in macrophages (Kawai et al., 1999; Takaoka et al., 2005). The TRIF-dependent gene induction is mainly regulated by IRF-3 (Sakaguchi et al., 2003; Yamamoto et al., 2003).

TLR-mediated gene expression regulates activation of not only innate immunity but also adaptive immunity, which provides antigen-specific responses against harmful pathogens (Iwasaki and Medzhitov, 2004; Pasare and Medzhitov, 2004). However, TLR-mediated activation of innate immunity, when in excess, triggers development of autoimmune disorders and inflammatory diseases, such as SLE, cardiomyopathy, atherosclerosis, diabetes mellitus, and inflammatory bowel diseases (Bjorkbacka et al., 2004; Eriksson et al., 2003; Kobayashi et al., 2003; Lang et al., 2005; Leadbetter et al., 2002; Michelsen et al., 2004). Excessive activation of TLR4 by LPS induces endotoxin shock, a serious systemic disorder with a high mortality rate. Therefore, TLR-dependent innate immune responses must be finely regulated, and underlying mechanisms are now being examined extensively (Liew et al., 2005). Several negative regulators of TLR-mediated signaling pathways have been proposed. Cytoplasmic molecules, such as an alternatively spliced short form of MyD88 (MyD88s), IRAK-M, SOCS1, A20, PI3-kinase, and TRIAD3A, are all involved in negative regulation of TLR pathways (Boone et al., 2004; Burns et al., 2003; Chuang and Ulevitch, 2004; Fukao et al., 2002; Kinjyo et al., 2002; Kobayashi et al., 2002; Nakagawa et al., 2002). Membrane bound SIGIRR, ST2, TRAILR, and RP105 are also implicated in these processes (Brint et al., 2004; Diehl et al., 2004; Divanovic et al., 2005; Wald et al., 2003).

TLR-dependent gene induction is also regulated by nuclear IκB proteins, such as IκBζ, Bcl-3, and IκBNS. IκBζ is indispensable for positive regulation of a subset of TLR-dependent genes, such as IL-6 and IL-12p40 (Yamamoto et al., 2004). In contrast, Bcl-3 and IκBNS seem to be involved in negative regulation of TLR-dependent gene induction. Bcl-3 was shown to be involved in selective inhibition of TLR-dependent TNF-α production (Kuwata et al., 2003; Wessells et al., 2004). An in vitro study indicated that IκBNS is induced by IL-10 or LPS and selectively inhibits IL-6 production in macrophages (Hirotani et al., 2005). Thus, nuclear IκB proteins differentially regulate TLR-dependent gene expression. However, the physiological role of IκBNS is still unclear.

In this study, we analyzed TLR-dependent inflammatory responses in IκBNS-deficient mice. We found that IκBNS is involved in selective inhibition of a subset of MyD88-dependent genes, including IL-6, IL-12p40, and IL-18. In IκBNS-deficient macrophages, LPS-induced activation of NF-κB was prolonged. Accordingly, IκBNS-deficient mice showed increased production of these cytokines accompanied by high sensitivity to LPS-induced endotoxin shock. Furthermore, IκBNS-deficient mice were highly susceptible to intestinal inflammation caused by disruption of the epithelial barrier. These findings indicate that IκBNS inhibits the induction of a group of TLR-dependent genes, thereby preventing excessive inflammation.

*Correspondence: ktakeda@bioreg.kyushu-u.ac.jp

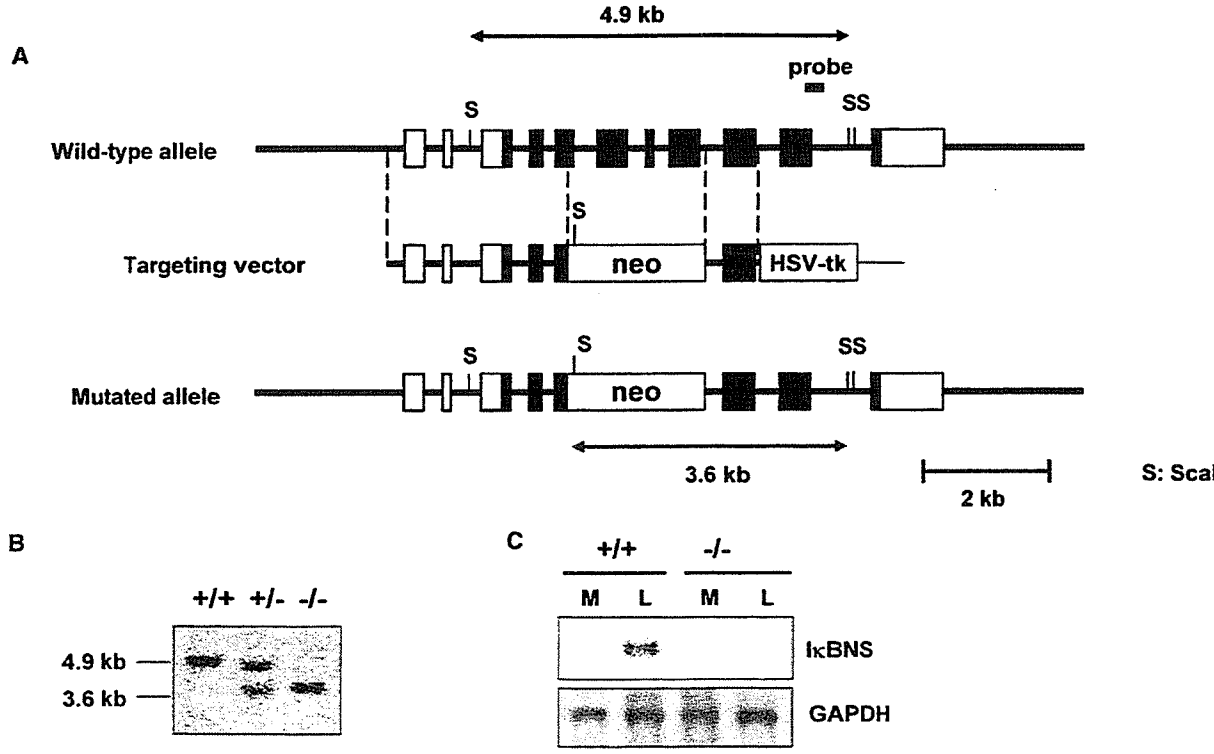

Figure 1. Targeted Disruption of the Mouse *Ikbns* Gene

(A) Maps of the IκBNS wild-type genome, targeting vector, and predicted targeted gene. Open and closed boxes denote the noncoding and coding exons, respectively. Restriction enzymes: S, ScaI.

(B) Southern blot analysis of offspring from the heterozygote intercrosses. Genomic DNA was extracted from mouse tails, digested with ScaI, electrophoresed, and hybridized with the probe indicated in (A). The approximate size of the wild-type band is 4.9 kb, and the mutated band is 3.6 kb.

(C) Peritoneal macrophages were cultured with or without 100 ng/ml LPS for 1 hr (L and M, respectively), and total RNA was extracted, electrophoresed, transferred to nylon membrane, and hybridized with the mouse IκBNS full-length cDNA probe. The same membrane was rehybridized with a GAPDH probe.

Results

Targeted Disruption of the IκBNS Gene

To study the functional role of IκBNS in TLR-dependent responses, a null mutation in the *Ikbns* allele was introduced through homologous recombination in embryonic stem (ES) cells (Figures 1A and 1B). IκBNS$^{-/-}$ mice were born alive and grew healthy until 20 weeks of age. We performed Northern blot analysis to confirm that the mutation causes inactivation of the *Ikbns* gene. LPS robustly induced IκBNS mRNA in wild-type macrophages, but not in IκBNS$^{-/-}$ macrophages (Figure 1C).

A previous report indicated that IκBNS is involved in negative selection of thymocytes (Fiorini et al., 2002). Therefore, we first analyzed lymphocyte composition in lymphoid organs such as thymus and spleen by flow cytometry (Figures S1A and S1B). Total cell number and CD4/CD8 or CD3/B220 populations in thymus and spleen were not altered in IκBNS$^{-/-}$ mice. Splenic T cells from IκBNS$^{-/-}$ mice showed similar levels of proliferative responses to IL-2 and IL-7 as did wild-type T cells. Moreover, IκBNS$^{-/-}$ T cells proliferated to almost equal degrees in response to anti-CD3 antibody compared to wild-type T cells (Figure S1C). These results indicate that T cell development and functions were generally unaffected in IκBNS$^{-/-}$ mice.

Increased IL-6 and IL-12p40 Production in IκBNS-Deficient Cells

Since IκBNS expression was induced within 1 hr of LPS stimulation in macrophages (Figure 1B), we stimulated peritoneal macrophages with various concentrations of LPS and analyzed for production of TNF-α and IL-6 (Figure 2A). In macrophages from IκBNS$^{-/-}$ mice, LPS-induced TNF-α production was comparable to wild-type cells, but IL-6 production was significantly increased. We then analyzed whether IκBNS$^{-/-}$ macrophages produce increased amounts of IL-6 in response to other TLR ligands, since IκBNS mRNA was induced by several TLR ligands as well as the TLR4 ligand LPS in a MyD88-dependent manner (Figure S2A). Peritoneal macrophages were stimulated with mycoplasmal lipopeptides (TLR6 ligand), Pam_3CSK_4 (TLR1 ligand), peptidoglycan (TLR2 ligand), and imiquimod (TLR7 ligand), and analyzed for production of TNF-α and IL-6 (Figure 2B). In response to these TLR ligands, the production of IL-6, but not TNF-α, was increased in IκBNS$^{-/-}$ mice. We next analyzed the response of bone marrow-derived dendritic cells (DCs). DCs from IκBNS$^{-/-}$ mice produced similar amounts of TNF-α and increased amounts of IL-6 in response to LPS compared to wild-type DCs (Figure 2C). In addition, DCs showed LPS-induced production of IL-12p40 and IL-12p70, and production of these

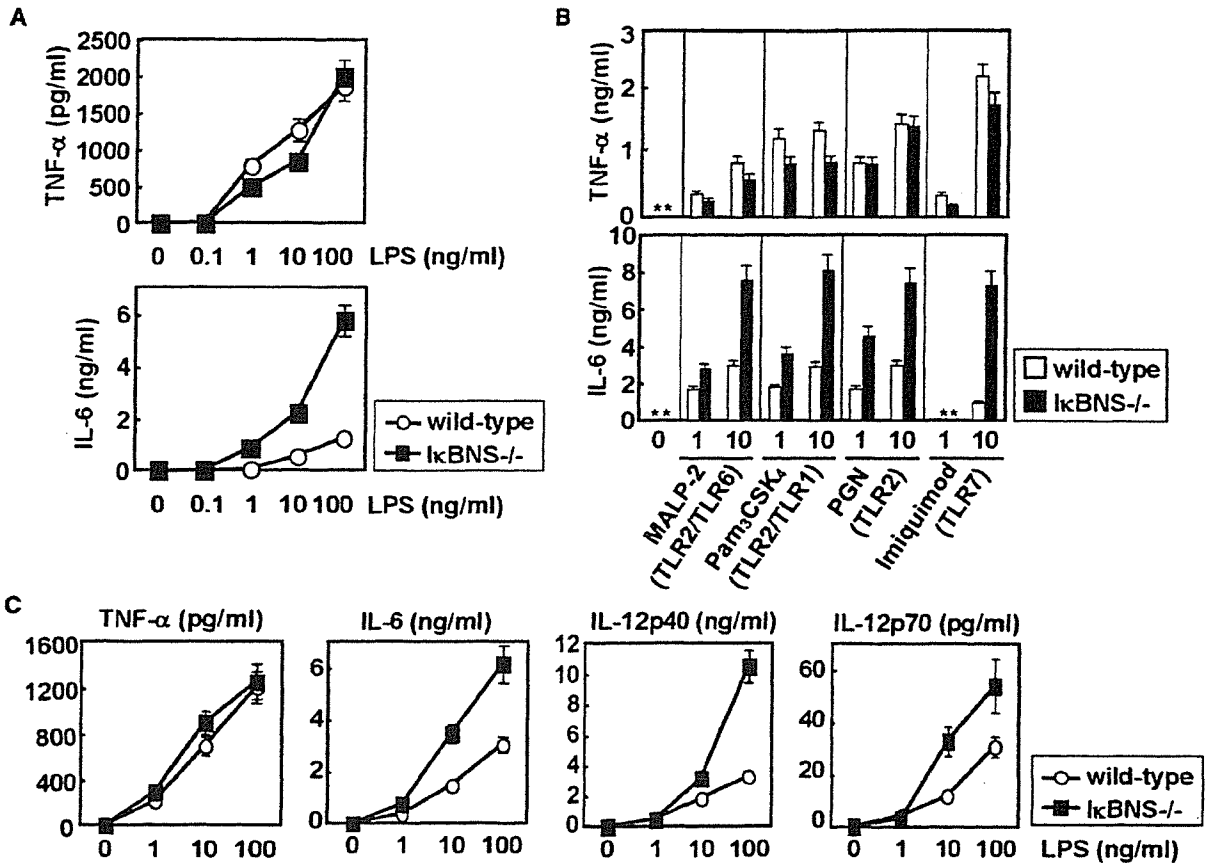

Figure 2. Increased Production of IL-6 and IL-12p40 in IκBNS$^{-/-}$ Macrophages and Dendritic Cells

(A) Peritoneal macrophages were stimulated with the indicated concentration of LPS for 24 hr. Concentrations of TNF-α and IL-6 in the culture supernantants were analyzed by ELISA. Data are mean ± SD of triplicate cultures in a single experiment, representative of three independent experiments.

(B) Peritoneal macrophages were cultured with 1 or 10 ng/ml of TLR6 ligand (MALP-2), 1 or 10 ng/ml TLR1 ligand (Pam_3CSK_4), 1 or 10 μg/ml TLR2 ligand (peptidoglycan; PGN), or 1 or 10 μg/ml TLR7 ligand (imiquimod) for 24 hr. Concentrations of TNF-α and IL-6 in the culture supernatants were analyzed by ELISA. "; not detected.

(C) Bone marrow-derived DCs were stimulated with the indicated concentration of LPS for 24 hr. Concentrations of TNF-α, IL-6, IL-12p40, and IL-12p70 in the culture supernatants were analyzed by ELISA. Data are mean ± SD of triplicate cultures in a single experiment, representative of three independent experiments.

cytokines was significantly increased in IκBNS$^{-/-}$ DCs. Bone marrow-derived DCs and splenic B cells were analyzed for LPS-induced surface expression of CD86 or MHC class II (Figure S2B). LPS-induced augmentation of surface expression of these molecules was not altered in IκBNS$^{-/-}$ mice. Thus, macrophages and DCs from IκBNS$^{-/-}$ mice showed selective increases in TLR-dependent production of IL-6 and IL-12p40.

Enhanced Induction of a Subset of TLR-Dependent Genes in IκBNS-Deficient Macrophages

We further analyzed LPS-induced mRNA expression of TLR-dependent genes in IκBNS$^{-/-}$ macrophages. Peritoneal macrophages were stimulated with LPS for 1, 3, or 5 hr, and total RNA was extracted. Then, mRNA expression of TNF-α and IL-6 was first analyzed by quantitative real-time RT-PCR (Figures 3A and 3B). LPS-induced TNF-α mRNA expression in IκBNS$^{-/-}$ macrophages was similar to wild-type cells. In the case of IL-6 mRNA, expression levels were comparable between wild-type and IκBNS$^{-/-}$ macrophages until 3 hr of LPS stimulation. After 3 hr, IL-6 mRNA levels decreased in wild-type cells. However, IκBNS$^{-/-}$ cells displayed further enhanced expression of IL-6 mRNA. TNF-α mRNA was robustly induced within 1 hr of LPS stimulation, and its expression promptly ceased in wild-type cells. In contrast, IL-6 mRNA expression was induced late compared to TNF-α. Because LPS-induced IκBNS mRNA expression showed similar patterns as TNF-α mRNA, we hypothesized that LPS-inducible IκBNS blocks mRNA expression of genes that are induced late (Figure 3C). Accordingly, we analyzed mRNA expression of other genes that are induced early (*Il-1β*, *Il-23p19*, or *Ikbz*) or late (*Il-12p40*, *Il-18*, or *Csf3*) in response to LPS. LPS-induced mRNA expression of *Il-1β* (IL-1β), *Il-23p19* (IL-23p19), and *Ikbz* (IκBζ) was similarly observed between wild-type and IκBNS$^{-/-}$ macrophages (Figure 3A). LPS-induced expression of *Il-12p40* (IL-12p40), *Il-18* (IL-18) and *Csf3* (G-CSF) was observed at normal levels in IκBNS$^{-/-}$ macrophages at the early phase of LPS stimulation (within 3 hr of LPS stimulation) (Figure 3B). However, at the late phase of LPS stimulation (after 3 hr of LPS stimulation), mRNA expression of these genes was significantly enhanced in

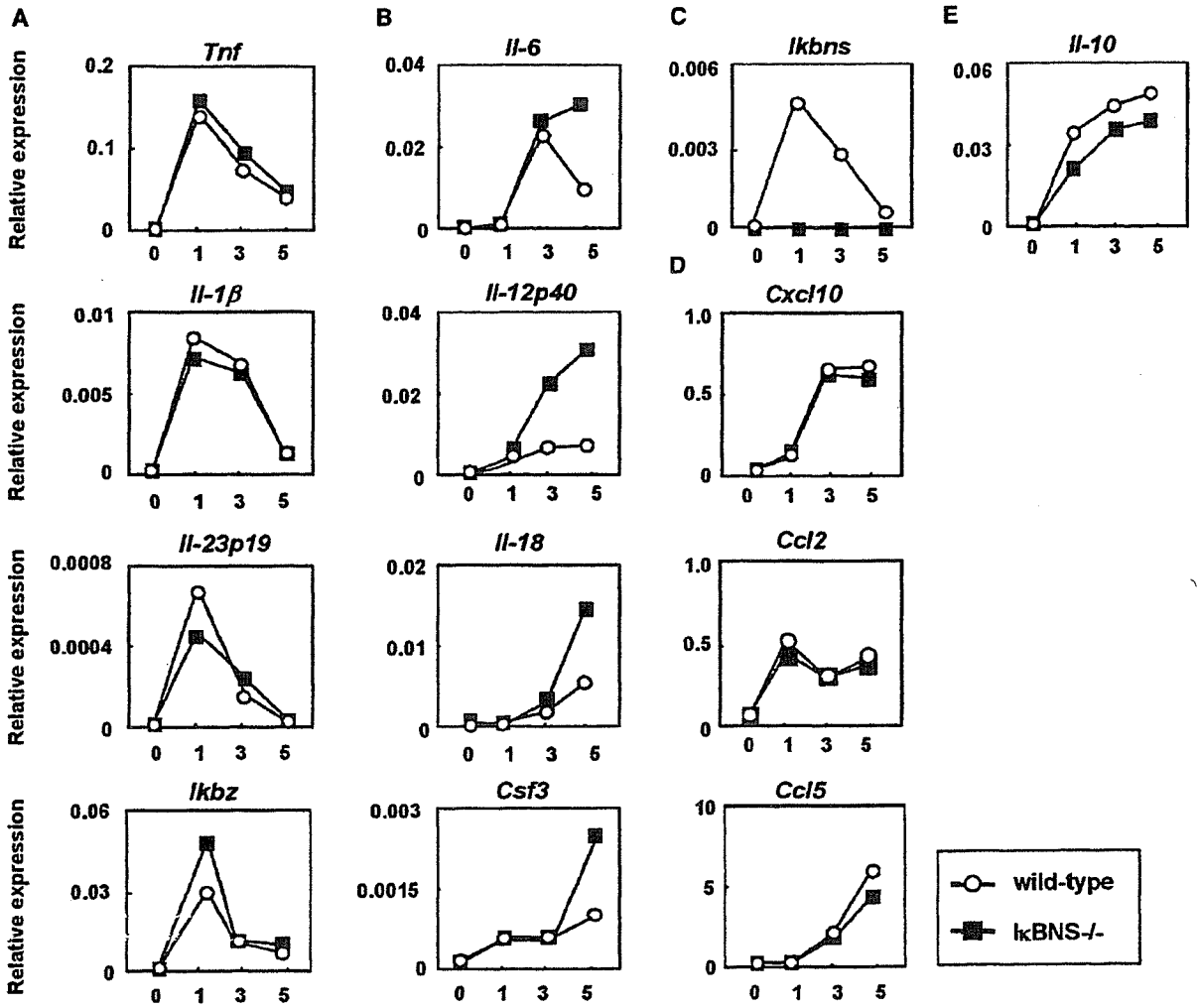

Figure 3. LPS-Induced Expression of Several TLR-Dependent Genes in IκBNS$^{-/-}$ Macrophages

Peritoneal macrophages from wild-type and IκBNS$^{-/-}$ mice were stimulated with 100 ng/ml LPS for the indicated periods. Total RNA was extracted, and then subjected to quantitative real-time RT-PCR analysis using primers specific for *Tnf*, *Il-1β*, *Il-23p19*, *Ikbz* (A), *Il-6*, *Il-12p40*, *Il-18*, *Csf3* (B), *Ikbns* (C), *Cxcl10*, *Ccl2*, *Ccl5* (D), and *Il-10* (E). The fold difference of each sample relative to EF-1α levels is shown. Representative of three independent experiments.

IκBNS$^{-/-}$ cells. We also analyzed LPS-induced expression of *Cxcl10* (IP-10), *Ccl2* (MCP-1), and *Ccl5* (RANTES), which are induced by the TRIF-dependent activation of IRF-3 (Figure 3D). LPS-induced expression of these genes was not altered in IκBNS$^{-/-}$ macrophages. An anti-inflammatory cytokine IL-10 is induced by TLR stimulation and thereby inhibits TLR-dependent gene induction (Moore et al., 2001). Therefore, we next addressed LPS-induced IL-10 mRNA expression (Figure 3E). LPS-induced IL-10 mRNA expression was comparable between wild-type and IκBNS$^{-/-}$ macrophages. In addition, LPS-induced production of IL-10 protein was not compromised in IκBNS$^{-/-}$ DCs (Figure S2C). These findings indicate that the enhanced LPS-induced expression of a subset of TLR-dependent genes was not due to the impaired IL-10 production in IκBNS$^{-/-}$ mice.

Prolonged NF-κB Activity in IκBNS-Deficient Cells

Gene expression of *Cxcl10* (IP-10), *Ccl2* (MCP-1), and *Ccl5* (RANTES) was mainly regulated by the transcription factor IRF-3 in the TRIF-dependent pathway, whereas TNF-α, IL-6, and IL-12p40 gene expression was mainly regulated by the MyD88-dependent activation of NF-κB (Akira and Takeda, 2004; Yamamoto et al., 2003). In addition, previous in vitro studies indicated that overexpression of IκBNS leads to compromised NF-κB activity through selective association of IκBNS with p50 subunit of NF-κB (Fiorini et al., 2002; Hirotani et al., 2005). Therefore, we next analyzed LPS-induced activation of NF-κB. LPS-induced degradation of IκBα was not compromised in IκBNS$^{-/-}$ macrophages (Figure S3A). Next, peritoneal macrophages or bone marrow-derived macrophages were stimulated with LPS and DNA binding activity was analyzed by EMSA (Figure 4A; Figure S3B). LPS stimulation resulted in enhanced DNA binding activity of NF-κB in both wild-type and IκBNS$^{-/-}$ macrophages to similar extents within 1 hr. After 1 hr of LPS stimulation, NF-κB activity decreased in wild-type cells. However, NF-κB activity sustained and even at 3 hr of LPS stimulation significant DNA binding activity was still observed in

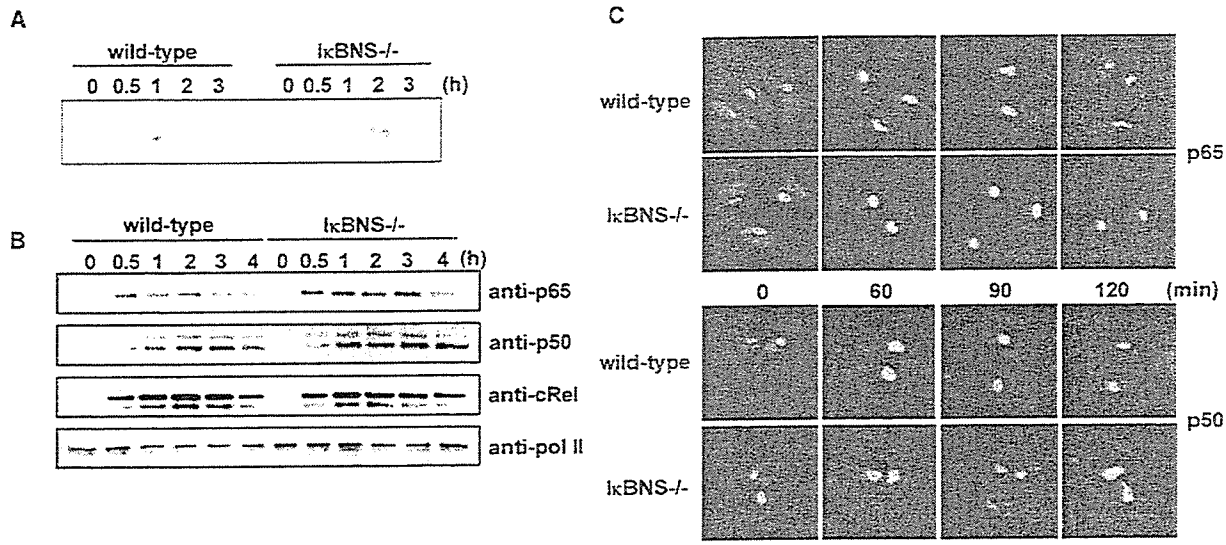

Figure 4. Persistent LPS-Induced Activation of NF-κB in IκBNS$^{-/-}$ Macrophages

(A) Peritoneal macrophages from wild-type and IκBNS$^{-/-}$ mice were stimulated with 100 ng/ml LPS. At the indicated time points, nuclear extracts were prepared, and NF-κB activation was analyzed by EMSA using a NF-κB specific probe.

(B) Peritoneal macrophages were stimulated with LPS. At the indicated time points, nuclear fractions were isolated and subjected to Western blotting using anti-p65 Ab, anti-p50 Ab, anti-cRel Ab, or anti-polII Ab.

(C) Macrophages were stimulated with LPS for the indicated periods. Then, cells were stained with anti-p65 Ab or anti-p50 Ab (red) as well as DAPI (blue), and analyzed by confocal microscopy. Merged images are shown.

IκBNS$^{-/-}$ cells. We next analyzed nuclear localization of NF-κB subunits. Peritoneal macrophages were stimulated with LPS for the indicated periods, and nuclear fractions were analyzed for expression of p65, p50, and c-Rel by immunoblotting (Figure 4B). In wild-type macrophages, nuclear translocation of p65 was observed within 30 min of LPS stimulation, and nuclear localized p65 gradually decreased thereafter. In contrast, nuclear localized p65 was still significantly observed even at 3 hr of LPS stimulation in IκBNS$^{-/-}$ cells. In addition, sustained nuclear localization of p50, but not c-Rel, was observed in IκBNS$^{-/-}$ macrophages (Figure 4B). Nuclear localization of NF-κB subunits was also analyzed by immunofluorescent staining of macrophages (Figure 4C). Without stimulation, p65 and p50 were localized in the cytoplasm, but not in the nucleus, in both wild-type and IκBNS$^{-/-}$ macrophages. LPS stimulation resulted in nuclear staining of both p65 and p50 at 1 hr. Nuclear staining of p65 and p50 gradually decreased after 1 hr of LPS stimulation and was only faintly observed at 2 hr of stimulation in wild-type cells. However, nuclear localization of p65 and p50 was still evident at 2 hr of LPS stimulation in IκBNS$^{-/-}$ cells. These findings indicate that LPS-induced NF-κB activity was prolonged in IκBNS$^{-/-}$ macrophages. NF-κB activity is terminated by degradation of promoter-bound p65 (Natoli et al., 2005; Saccani et al., 2004). We used RAW264.7 macrophage cell line and performed pulse-chase experiments with ^{35}S-labeled amino acids to analyze p65 turnover (Figure S3C). In these cells, labeled p65 was accumulated into the nucleus until 2 hr of LPS stimulation, and then p65 was degraded. In RAW cells constitutively expressing IκBNS, nuclear accumulation of labeled p65 was similarly observed until 1 hr of LPS stimulation. However, the p65 turnover was observed more rapidly and labeled p65 disappeared at 2 hr after LPS stimulation (Figure S3C). These findings indicate that IκBNS mediates the degradation of p65. The MyD88-dependent pathway mediates activation of MAP kinase cascades as well as NF-κB activation. Therefore, LPS-induced phosphorylation of p38, ERK1, ERK2, and JNK was analyzed by Western blotting (Figure S3D). LPS-induced activation of these MAP kinases was not compromised in IκBNS$^{-/-}$ macrophages.

Regulation of p65 Activity at the IL-6 Promoter by IκBNS

We next addressed how IκBNS selectively downregulates induction of genes that are induced late. We utilized the IL-6 and TNF-α promoters, which are representatives of genes activated late and early, respectively. Wild-type macrophages were stimulated with LPS and analyzed for recruitment of endogenous IκBNS to the promoters by chromatin immunoprecipitation (ChIP) assay (Figure 5A). Consistent with previous findings using IκBNS overexpressing macrophage cell lines (Hirotani et al., 2005), endogenous IκBNS was recruited to the IL-6 promoter, but not the TNF-α promoter, in LPS-stimulated macrophages. We next addressed LPS-induced recruitment of p65 to the promoters in wild-type and IκBNS$^{-/-}$ macrophages (Figure 5B). Recruitment of p65 to the TNF-α promoter peaked at 1 hr of LPS stimulation and gradually decreased thereafter in a similar manner in both wild-type and IκBNS$^{-/-}$ cells. Recruitment of p65 to the IL-6 promoter was observed to similar extents until 3 hr of LPS stimulation in wild-type and IκBNS$^{-/-}$ macrophages. After that, it decreased in wild-type macrophages. In contrast, p65 recruitment was still evident, rather enhanced, even after 5 hr of LPS stimulation in IκBNS$^{-/-}$ macrophages. Thus, p65 activity at

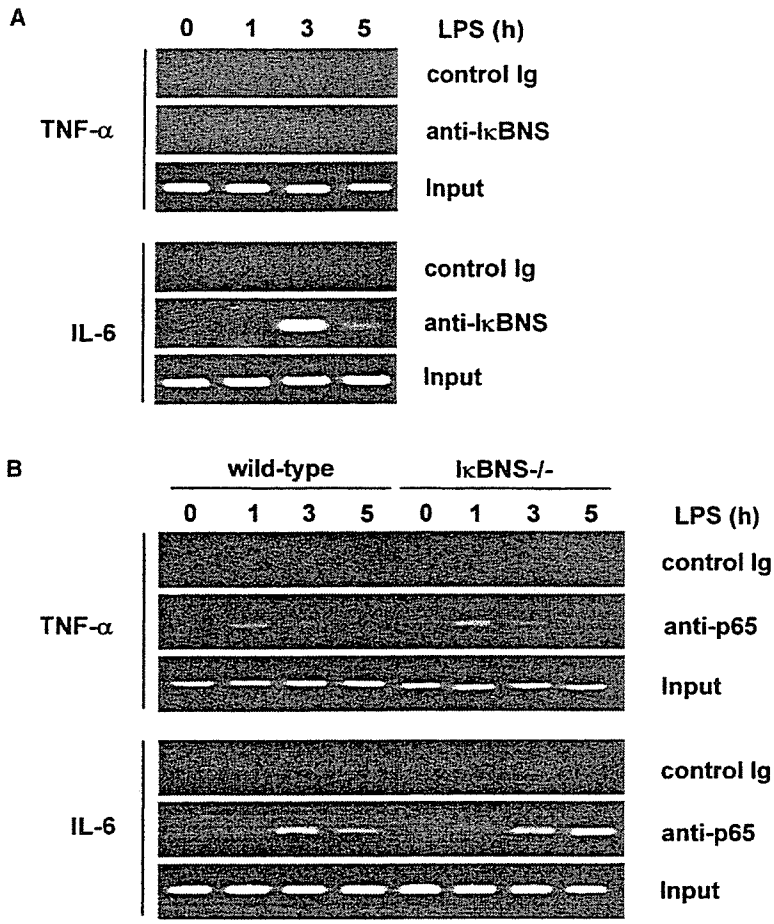

Figure 5. IκBNS Regulation of p65 Activity at the IL-6 Promoter

(A) Wild-type bone marrow-derived macrophages were stimulated with 100 ng/ml of LPS for the indicated periods, and chromatin immunoprecipitation (ChIP) assay was performed with anti-IκBNS Ab or control Ig. The immunoprecipitated TNF-α promoter (upper panel) or IL-6 promoter (lower panel) was analyzed by PCR with promoter-specific primers. PCR amplification of the total input DNA in each sample is shown (Input). Representative of three independent experiments. The same result was obtained when peritoneal macrophages were used.

(B) Macrophages from wild-type or IκBNS$^{-/-}$ mice were stimulated with LPS for the indicated periods. Then, ChIP assay was performed with anti-p65 Ab or control Ig. The immunoprecipitated TNF-α promoter (upper panel) or IL-6 promoter (lower panel) was analyzed by PCR with promoter-specific primers. Representative of three independent experiments.

the IL-6 promoter, but not at the TNF-α promoter, was prolonged in LPS-stimulated IκBNS$^{-/-}$ macrophages. Taken together, these findings indicate that TLR-inducible IκBNS is responsible for termination of NF-κB activity through its recruitment to specific promoters.

High Sensitivity to LPS-Induced Endotoxin Shock in IκBNS-Deficient Mice

To study the in vivo role of IκBNS, we examined LPS-induced endotoxin shock. Intraperitoneal injection of LPS resulted in marked increases in serum concentrations of TNF-α, IL-6, and IL-12p40 (Figure 6A). TNF-α level was comparable between wild-type and IκBNS$^{-/-}$ mice, which rapidly peaked at around 1.5 hr of LPS administration. In the case of IL-6 and IL-12p40 levels, concentrations of both cytokines were almost equally elevated within 3 hr of LPS injection. After 3 hr, levels of both cytokines gradually decreased in wild-type mice. However, concentrations of IL-6 and IL-12p40 sustained, rather enhanced, in IκBNS$^{-/-}$ mice after 3 hr. Thus, persistently high concentrations of LPS-induced serum IL-6 and IL-12p40 were observed in IκBNS$^{-/-}$ mice. Furthermore, high sensitivity to LPS-induced lethality was observed in IκBNS$^{-/-}$ mice (Figure 6B). All IκBNS$^{-/-}$ mice died within 4 days of LPS challenge at a dose of which almost all wild-type mice survived over 4 days. These findings indicate that IκBNS$^{-/-}$ mice are highly sensitive to LPS-induced endotoxin shock.

High Susceptibility to DSS-Induced Colitis in IκBNS$^{-/-}$ Mice

In a previous report, IκBNS was shown to be constitutively expressed in macrophages residing in the colonic lamina propria, which explains one of the mechanisms for hyporesponsiveness to TLR stimulation in these cells (Hirotani et al., 2005). Therefore, we next stimulated CD11b^{+} cells isolated from the colonic lamina propria with LPS and analyzed for production of TNF-α and IL-6 (Figure S4). In CD11b^{+} cells from wild-type mice, LPS-induced production of these cytokines was not significantly observed. In cells from IκBNS$^{-/-}$ mice, IL-6 production was increased even in the absence of stimulation, and LPS stimulation led to markedly enhanced production of IL-6, but not TNF-α. In the next experiment, in order to expose these cells to microflora and cause intestinal inflammation, mice were orally administered with dextran sodium sulfate (DSS), which is toxic to colonic epithelial cells and therefore disrupts the epithelial cell barrier (Kitajima et al., 1999). IκBNS$^{-/-}$ mice showed more severe weight loss compared with wild-type mice (Figure 7A). Histological analyses of the colon indicated that the inflammatory lesions were more severe and more extensive in IκBNS$^{-/-}$ mice (Figures 7B and 7C). Thus, IκBNS$^{-/-}$ mice are highly susceptible to intestinal inflammation. Th1-oriented CD4^{+} T cell response was shown to be associated with DSS colitis (Strober et al., 2002). Therefore, we analyzed IFN-γ

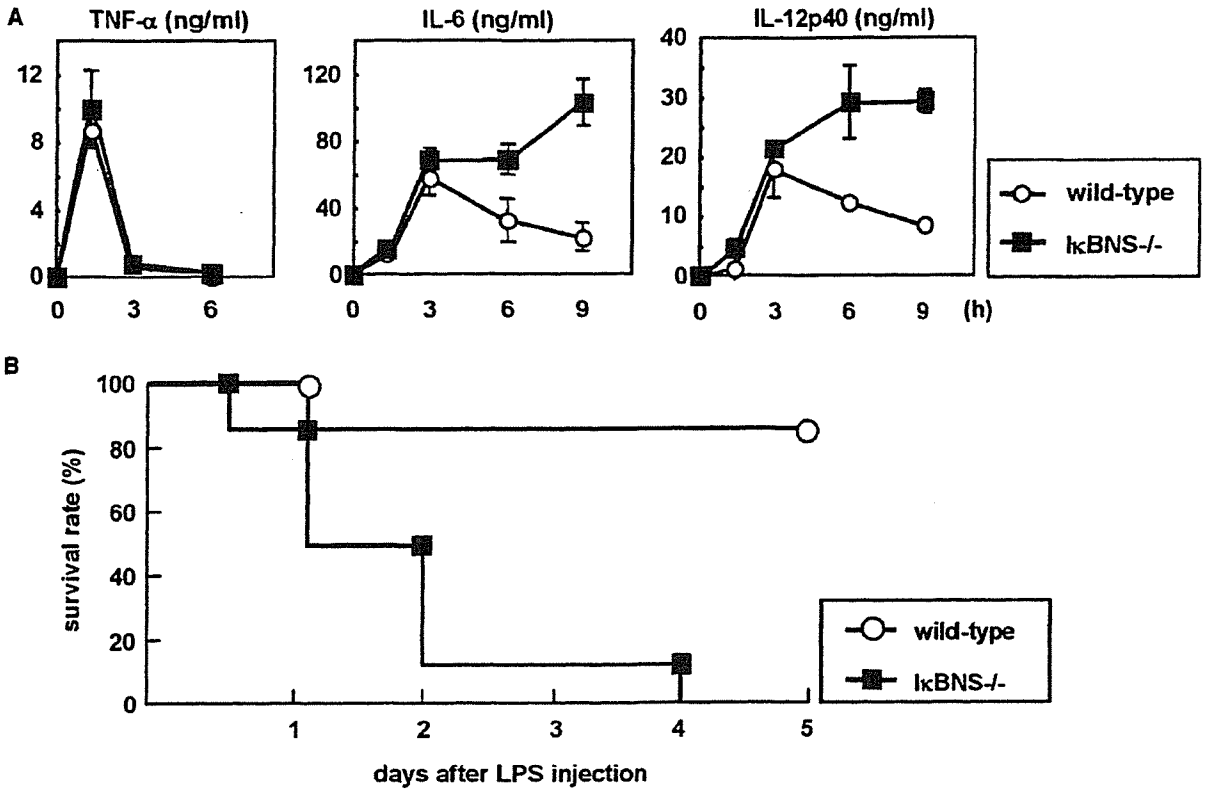

Figure 6. High Susceptibility to LPS-Induced Endotoxin Shock in IκBNS$^{-/-}$ Mice

Age-matched wild-type (n = 6) and IκBNS−/− (n = 6) mice were intraperitoneally injected with LPS (1 mg). (A) Sera were taken at 1.5, 3, 6, and 9 hr after LPS injection. Serum concentrations of TNF-α, IL-6, and IL-12p40 were determined by ELISA. Results are shown as mean ± SD of serum samples from six mice. (B) Survival was monitored for 5 days.

production from splenic CD4$^+$ T cells of wild-type and IκBNS$^{-/-}$ mice before and after DSS administration (Figure 7D). DSS administration led to a mild increase in IFN-γ production in wild-type mice. In nontreated IκBNS$^{-/-}$ mice, IFN-γ production was slightly increased compared with nontreated wild-type mice. In DSS-fed IκBNS$^{-/-}$ mice, a significant increase in IFN-γ production was observed compared to DSS-fed wild-type mice. These results indicate that IκBNS$^{-/-}$ mice are susceptible to intestinal inflammation caused by exposure to microflora.

Discussion

In the present study, we characterized the physiological function of IκBNS. Induced by TLR stimulation, IκBNS is involved in termination of NF-κB activity and thereby inhibits a subset of TLR-dependent genes that are induced late through MyD88-dependent NF-κB activation. Accordingly, IκBNS$^{-/-}$ mice show sustained production of IL-6 and IL-12p40, resulting in high susceptibility to LPS-induced endotoxin shock. Furthermore, IκBNS$^{-/-}$ mice are susceptible to intestinal inflammation accompanied by enhanced Th1 responses.

IκBNS was originally identified as a molecule that mediates negative selection of thymocytes (Fiorini et al., 2002). However, IκBNS$^{-/-}$ mice did not show any defect in T cell development. Requirement of IκBNS in negative selection of thymocytes should be analyzed precisely using peptide-specific TCR transgenic mice, such as mice bearing the H-Y TCR, in the future (Kisielow et al., 1988).

Recent studies have established that TLR-dependent gene induction is regulated mainly by NF-κB and IRF families of transcription factors (Akira and Takeda, 2004; Honda et al., 2005; Takaoka et al., 2005). In TLR4 signaling, the TRIF-dependent pathway is responsible for induction of IFN-β and IFN-inducible genes through activation of IRF-3, whereas the MyD88-dependent pathway mediates induction of several NF-κB dependent genes (Beutler, 2004). A study with mice lacking IκBζ, another member of nuclear IκB proteins, has demonstrated that the MyD88-dependent genes are divided into at least two types; one is induced early and independent of IκBζ, and another is induced late and dependent on IκBζ (Yamamoto et al., 2004). The IκBζ-regulated genes include IL-6, IL-12p40, IL-18, and G-CSF, which are all upregulated in LPS-stimulated IκBNS$^{-/-}$ macrophages. Thus, IκBNS seems to possess a function quite opposite to IκBζ. IκBNS is most structurally related to IκBζ (Fiorini et al., 2002; Hirotani et al., 2005). But, IκBζ has an additional N-terminal structure, which seemingly mediates the induction of target genes (Motoyama et al., 2005). Thus, nuclear IκB proteins IκBζ and IκBNS positively and negatively regulate a subset of TLR-induced NF-κB-dependent genes, respectively.

Recently, negative regulation of TLR-dependent gene induction was extensively analyzed (Liew et al., 2005).

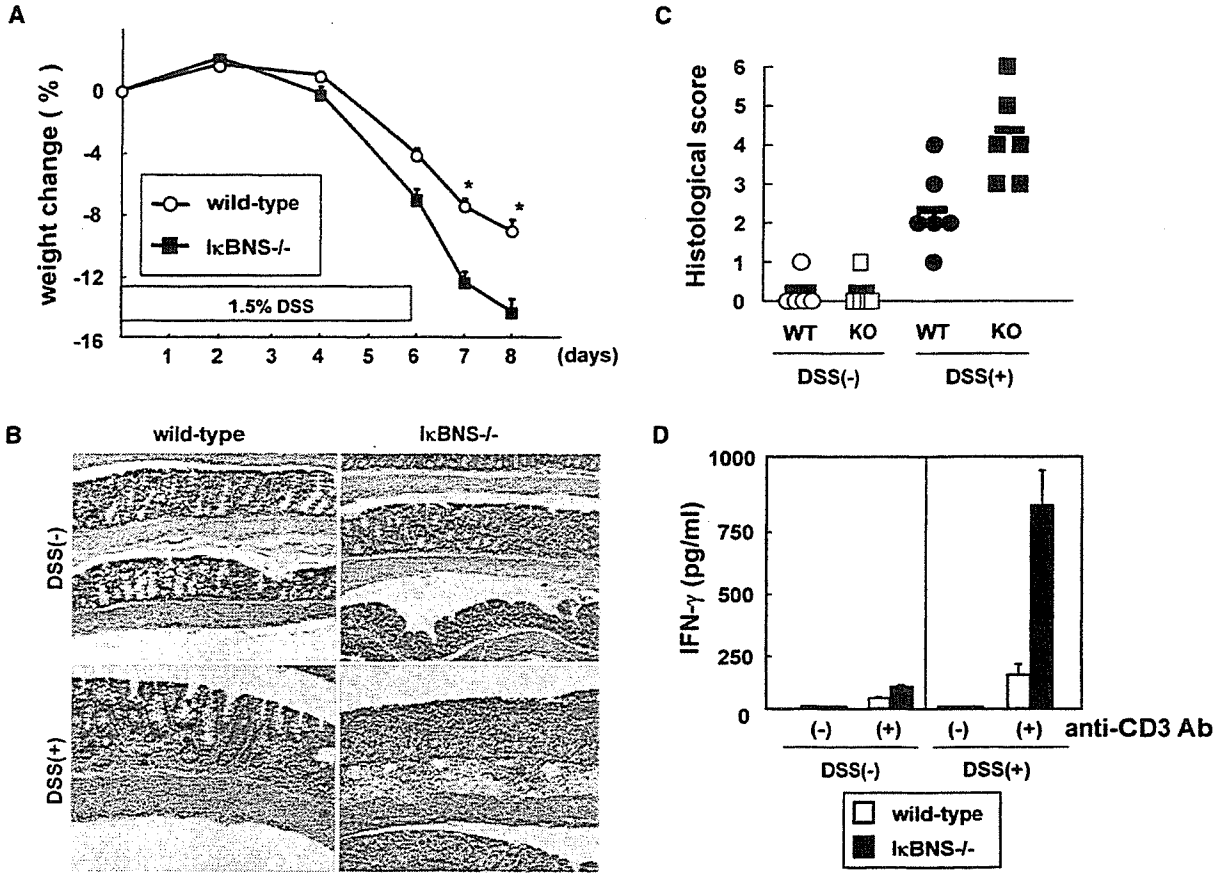

Figure 7. High Susceptibility to DSS Colitis in IκBNS$^{-/-}$ Mice

(A) Wild-type (n = 15) and IκBNS$^{-/-}$ mice (n = 15) were given 1.5% DSS in drinking water for 6 days and weighed everyday. Data are mean ± SD. *, $p < 0.05$.

(B) Histologic examination of the colons of wild-type and IκBNS$^{-/-}$ mice before or 9 days after initiation of DSS administration. H&E staining is shown. Representative of six mice examined. Magnification, 20×.

(C) The colitis scores shown for individual wild-type (circle) and IκBNS$^{-/-}$ mice (square) before (open) and after (closed) DSS treatment were total scores for individual sections as described in the Experimental Procedures section. Mean score for each group is also shown (black bar).

(D) CD4$^+$ T cells were purified from spleen of wild-type or IκBNS$^{-/-}$ mice either treated or nontreated with DSS. Then, CD4$^+$ T cells were cultured in the presence or absence of plate bound anti-CD3 Ab for 24 hr. Concentration of IFN-γ in the culture supernatants was measured by ELISA.

So far, characterized negative regulators are mainly involved in blockade of TLR signaling pathways in the cytoplasm or on the cell membrane. Accordingly, these negative regulators globally inhibit TLR-dependent gene induction. The nuclear IκB protein IκBNS is unique in that this molecule negatively regulates induction of a set of TLR-dependent genes by directly affecting NF-κB activity in the nucleus. Thus, TLR-dependent innate immune responses are regulated through a variety of mechanisms.

IκBNS-mediated inhibition of a set of TLR-dependent genes is probably explained by recruitment of IκBNS to the specific promoters. IκBNS was recruited to the IL-6 promoter, but not to the TNF-α promoter. In addition, LPS-induced recruitment of p65 to the TNF-α promoter was observed within 1 hr, whereas p65 recruitment to the IL-6 promoter was observed late, indicating that NF-κB activity was differentially regulated at both promoters. NF-κB activity at the TNF-α promoter is regulated in an IκBNS-independent manner, whereas the activity at the IL-6 promoter was IκBNS-dependent. Indeed, p65 recruitment to the TNF-α promoter was observed similarly in wild-type and IκBNS$^{-/-}$ macrophages, but the recruitment to the IL-6 promoter was sustained in IκBNS$^{-/-}$ cells. Previous reports indicate that IκBNS selectively associates with p50 subunit of NF-κB and affects NF-κB DNA binding activity (Fiorini et al., 2002; Hirotani et al., 2005). Consistent with these observations, IκBNS$^{-/-}$ macrophages showed prolonged LPS-induced NF-κB DNA binding activity and nuclear localization of p65. Taken together, these findings indicate that IκBNS, which is rapidly induced by TLR stimulation, might be recruited to gene promoters through association with p50, and contribute to termination of NF-κB activity. Termination of NF-κB activity has been shown to be induced by IKKα-mediated degradation of promoter-bound p65 (Lawrence et al., 2005). However, consistent with a recent report, we were not able to detect LPS-induced degradation of p65 in peritoneal macrophages and bone marrow-derived macrophages (Li et al., 2005). However, we could detect LPS-induced p65 degradation in the RAW264.7 macrophage cell line. In these cells, when constitutively expressed IκBNS, LPS-induced p65 turnover was

accelerated, indicating that IκBNS is involved in the degradation of promoter-bound p65. In the case of the TNF-α promoter, it is possible that NF-κB activity is already terminated when IκBNS expression is induced, and therefore IκBNS is no longer recruited to the TNF-α promoter. Alternatively, an unidentified mechanism that regulates selective recruitment of IκBNS to gene promoters might exist. The mechanisms by which IκBNS is recruited to the specific promoters through association with p50 remain unclear and would be a subject of further investigation.

Analyses of IκBNS$^{-/-}$ mice further highlighted the in vivo functions of IκBNS in limiting systemic and intestinal inflammation. IκBNS$^{-/-}$ mice succumbed to systemic LPS-induced endotoxin shock possibly due to sustained production of several TLR-dependent gene products such as IL-6 and IL-12p40. Furthermore, IκBNS$^{-/-}$ mice are more susceptible to intestinal inflammation induced by disruption of the epithelial barrier. Abnormal activation of innate immune cells caused by deficiency of IL-10 or Stat3 leads to spontaneous development of colonic inflammation (Kobayashi et al., 2003; Kuhn et al., 1993; Takeda et al., 1999). IκBNS$^{-/-}$ mice did not develop chronic colitis spontaneously until 20 week-old of age (our unpublished data). In Stat3 mutant mice, TLR-dependent production of proinflammatory cytokines increased over 10-fold compared to wild-type cells, which might contribute to the spontaneous intestinal inflammation (Takeda et al., 1999). In IκBNS$^{-/-}$ mice, increase in TLR-dependent production of proinflammatory cytokines such as IL-6 and IL-12p40 was mild compared to Stat3 mutant mice. In this case, the colonic epithelial barrier might contribute to prevention of excessive inflammatory responses in IκBNS$^{-/-}$ mice. However, when the barrier function of epithelial cells was disrupted by administration of DSS, IκBNS$^{-/-}$ mice suffered from severe intestinal inflammation accompanied by enhanced Th1 responses. IκBNS was shown to be expressed in CD11b^{+} cells residing in the colonic lamina propria (Hirotani et al., 2005). Therefore, in the absence of IκBNS, exposure of innate immune cells to intestinal microflora might result in increased or sustained production of proinflammatory cytokines such as IL-12p40, which induces exaggerated intestinal inflammation and Th1 cell development. Thus, IκBNS is responsible for the prevention of uncontrolled inflammatory responses in vivo.

In this study, we have shown that IκBNS is a selective inhibitor of TLR-dependent genes possibly through termination of NF-κB activity. Furthermore, IκBNS was responsible for prevention of inflammation through inhibition of persistent proinflammatory cytokine production. Future study that discloses the precise molecular mechanisms by which the nuclear IκB protein selectively inhibits TLR-dependent genes will provide basis for the development of new therapeutic strategies to a variety of inflammatory diseases.

Experimental Procedures

Generation of IκBNS-Deficient Mice

The *Ikbns* gene consists of eight exons (Figure 1A). The targeting vector was designed to replace a 1.8 kb fragment containing exons 5–8 of the *Ikbns* gene with a neomycin-resistance gene (*neo*). A short arm and a long arm of the homology region from the E14.1 ES genome were amplified by PCR. A herpes simplex virus thymidine kinase gene (HSV-TK) was inserted into the 3′ end of the vector. After the targeting vector was electroporated into ES cells, G418 and gancyclovir doubly resistant clones were selected and screened for homologous recombination by PCR and verified by Southern blot analysis using the probe indicated in Figure 1A. Two independently identified targeted ES clones were microinjected into C57BL/6 blastocysts. Chimeric mice were mated with C57BL/6 female mice, and heterozygous F1 progenies were intercrossed to obtain IκBNS$^{-/-}$ mice. Mice from these independent ES clones displayed identical phenotypes. All animal experiments were conducted according to guidelines of Animal Care and Use Committee at Kyushu University.

Reagents

LPS (*E. coli* 055:B5) was purchased from Sigma. Peptidoglycan was from Fluca. Pam_3CSK_4, MALP-2, and imiquimod were from Invivogen. Antibodies against p65 (C-20; sc-372), p50 (H-119; sc-7178 or NLS; sc-114), c-Rel (C; sc-71), and RNA polymerase II (H-224; sc-9001) were purchased from Santa Cruz. Rabbit anti-IκBNS Ab was generated against synthetic peptide (1-MEDSLDTRLY PEPSLSQVC-18) corresponding to N-terminal region of mouse IκBNS (MBL, Nagoya, Japan), and anti-IκBNS serum was affinity-purified using a column containing peptide-conjugated Sepharose 4B.

Preparation of Macrophages and Dendritic Cells

For isolation of peritoneal macrophages, mice were intraperitoneally injected with 2 ml of 4% thioglycollate medium (Sigma). Peritoneal exudate cells were isolated from the peritoneal cavity 3 days post injection. Cells were incubated for 2 hr and washed three times with HBSS. Remaining adherent cells were used as peritoneal macrophages for the experiments. To prepare bone marrow-derived macrophages, bone marrow cells were prepared from femora and tibia and passed through nylon mesh. Then cells were cultured in RPMI 1640 medium supplemented with 10% FCS, 100 μM 2-ME, and 10 ng/ml M-CSF (GenzymeTechne). After 6–8 days, the cells were used as macrophages for the experiments. Bone marrow-derived DCs were prepared by culturing bone marrow cells in RPMI 1640 medium supplemented with 10% FCS, 100 μM 2-ME, and 10 ng/ml GM-CSF (GenzymeTechne). After 6 days, the cells were used as DCs.

Measurement of Cytokine Production

Peritoneal macrophages or DCs were stimulated with various TLR ligands for 24 hr. Culture supernatants were collected and analyzed for TNF-α, IL-6, IL-12p40, IL-12p70, or IL-10 production with enzyme-linked immunosorbent assay (ELISA). Mice were intravenously injected with 1mg of LPS and bled at the indicated periods. Serum concentrations of TNF-α, IL-6, and IL-12p40 were determined by ELISA. ELISA kits were purchased from GenzymeTechne and R&D Systems. For measurement of IFN-γ, CD4^{+} T cells were purified from spleen cells using CD4 microbeads (Miltenyi Biotec) and stimulated by plate bound anti-CD3ε antibody (145-2C11, BD PharMingen) for 24 hr. Concentrations of IFN-γ in the supernatants were determined by ELISA (GenzymeTechne).

Quantitative Real-Time RT-PCR

Total RNA was isolated with TRIzol reagent (Invitrogen, Carlsbad, CA), and 2 μg of RNA was reverse transcribed using M-MLV reverse transcriptase (Promega, Madison, WI) and oligo (dT) primers (Toyobo, Osaka, Japan) after treatment with RQ1 DNase I (Promega). Quantitative real-time PCR was performed on an ABI 7700 (Applied Biosystems, Foster City, CA) using TaqMan Universal PCR Master Mix (Applied Biosystems). All data were normalized to the corresponding elongation factor-1α (EF-1α) expression, and the fold difference relative to the EF-1α level was shown. Amplification conditions were: 50°C (2 min), 95°C (10 min), 40 cycles of 95°C (15 s), and 60°C (60 s). Each experiment was performed independently at least three times, and the results of one representative experiment are shown. All primers were purchased from Assay on Demand (Applied Biosystems).

Electrophoretic Mobility Shift Assay

Macrophages were stimulated with 100 ng/ml LPS for the indicated periods. Then, nuclear proteins were extracted, and incubated with an end-labeled, double-stranded oligonucleotide containing an NF-κB binding site of the IL-6 promoter in 25 μl of binding buffer (10 mM HEPES-KOH, [pH 7.8], 50 mM KCl, 1 mM EDTA [pH 8.0], 5 mM $MgCl_2$ and 10% glycerol) for 20 min at room temperature and loaded on a native 5% polyacrylamide gel. The DNA-protein complexes were visualized by autoradiography.

Western Blotting

Cells were lysed with RIPA buffer (50 mM Tris-HCl [pH 7.5], 150 mM NaCl, 1% Triton X-100, 0.5% Na-deoxycholate) containing protease inhibitors (Complete Mini; Roche). The lysates were separated on SDS-PAGE and transferred to PVDF membrane. The membranes were incubated with anti-IκBα Ab, anti-ERK Ab, anti-p38 Ab, anti-JNK Ab (Santa Cruz Biotechnology), anti-phospho-p38 Ab, anti-phospho-ERK Ab, or anti-phospho-JNK Ab (Cell Signaling Technology). Bound Abs were detected with SuperSignal West Pico Chemiluminescent Substrate (Pierce).

Immunofluorescence Staining

Macrophages were stimulated with 100 ng/ml LPS for the indicated periods, washed with Tris-buffered saline (TBS), and fixed with 3.7% formaldehyde in TBS for 15 min at room temperature. After permeabilization with 0.2% Triton X-100, cells were washed with TBS and incubated with 10 ng/ml of a rabbit anti-p50 or anti-p65 Ab (Santa Cruz Biotechnology) in TBS containing 1% bovine serum albumin, followed by incubation with Alexa Fluor 594-conjugated goat anti-rabbit immunoglobulin G (IgG; Molecular Probes, Eugene, OR). To stain the nucleus, cells were cultured with 0.5 μg/ml 4, 6-diamidino-2-phenylindole (DAPI; Wako, Osaka, Japan). Stained cells were analyzed using an LSM510 model confocal microscope (Carl Zeiss, Oberkochem, Germany).

Chromatin Immunoprecipitation

Chromatin immunoprecipitation (ChIP) was performed essentially with a described protocol (Upstate Biotechnology, Lake Placid, NY). In brief, peritoneal macrophages from wild-type and $I\kappa BNS^{-/-}$ mice were stimulated with 100 ng/ml LPS for 1, 3, or 5 hr, and then fixed with formaldehyde for 10 min. The cells were lysed, sheared by sonication using Bioruptor (CosmoBio), and incubated overnight with specific antibody followed by incubation with protein A-agarose saturated with salmon sperm DNA (Upsate Biotechnology). Precipitated DNA was analyzed by quantitative PCR (35 cycles) using primers 5′- CCCCAGATTGCCACAGAATC -3′ and 5′- CCAGT GAGTGAAAGGGACAG -3′ for the TNF-α promoter and 5′- TGTGTG TCGTCTGTCATGCG-3′ and 5′- AGCTACAGACATCCCCAGTCTC -3′ for the IL-6 promoter.

Induction of DSS Colitis

Mice received 1.5% (wt/vol) DSS (40,000 kDa; ICN Biochemicals), ad libitum, in their drinking water for 6 days, then switched to regular drinking water. The amount of DSS water drank per animal was recorded and no differences in intake between strains were observed. Mice were weighed for the determination of percent weight change. This was calculated as: percentage weight change = (weight at day X-day 0/weight at day 0) × 100. Statistical significance was determined by paired Student's t test. Differences were considered to be statistically significant at $p < 0.05$.

Histological Analysis

Colon tissues were fixed in 4% paraformaldehyde, rolled up, and embedded in paraffin in a Swiss roll orientation such that the entire length of the intestinal tract could be identified on single sections. After sectioning, the tissues were dewaxed in ethanol, rehydrated, and stained hematoxylin and eosin to study histological changes after DSS-induced damage. Histological scoring was performed in a blinded fashion by a pathologist, with a combined score for inflammatory cell infiltration (score, 0–3) and tissue damage (score, 0–3) (Araki et al., 2005). The presence of occasional inflammatory cells in the lamina propria was assigned a value of 0; increased numbers of inflammatory cells in the lamina propria as 1; confluence of inflammatory cells, extending into the submucosa, as 2; and transmural extension of the infiltrate as 3. For tissue damage, no mucosal damage was scored as 0; discrete lymphoepithelial lesions were scored as 1; surface mucosal erosion or focal ulceration was scored as 2; and extensive mucosal damage and extension into deeper structures of the bowel wall were scored as 3. The combined histological score ranged from 0 (no changes) to 6 (extensive cell infiltration and tissue damage).

Supplemental Data

Supplemental Data include four figures and are available with this article online at http://www.immunity.com/cgi/content/full/24/1/41/DC1/.

Acknowledgments

We thank Y. Yamada, K. Takeda, M. Otsu, and N. Kinoshita for technical assistance; M. Yamamoto and S. Akira for providing us with reagents, P. Lee for critical reading of the manuscript, and M. Kurata for secretarial assistance. This work was supported by grants from the Special Coordination Funds of the Ministry of Education, Culture, Sports, Science and Technology; the Uehara Memorial Foundation; the Mitsubishi Foundation; the Takeda Science Foundation; the Tokyo Biochemical Research Foundation; the Kowa Life Science Foundation; the Osaka Foundation for Promotion of Clinical Immunology; and the Sankyo Foundation of Life Science.

Received: July 15, 2005
Revised: September 16, 2005
Accepted: November 16, 2005
Published: January 17, 2006

References

Akira, S., and Takeda, K. (2004). Toll-like receptor signalling. Nat. Rev. Immunol. *4*, 499–511.

Araki, A., Kanai, T., Ishikura, T., Makita, S., Uraushihara, K., Iiyama, R., Totsuka, T., Takeda, K., Akira, S., and Watanabe, M. (2005). MyD88-deficient mice develop severe intestinal inflammation in dextran sodium sulfate colitis. J. Gastroenterol. *40*, 16–23.

Beutler, B. (2004). Inferences, questions and possibilities in Toll-like receptor signalling. Nature *430*, 257–263.

Bjorkbacka, H., Kunjathoor, V.V., Moore, K.J., Koehn, S., Ordija, C.M., Lee, M.A., Means, T., Halmen, K., Luster, A.D., Golenbock, D.T., and Freeman, M.W. (2004). Reduced atherosclerosis in MyD88-null mice links elevated serum cholesterol levels to activation of innate immunity signaling pathways. Nat. Med. *10*, 416–421.

Boone, D.L., Turer, E.E., Lee, E.G., Ahmad, R.C., Wheeler, M.T., Tsui, C., Hurley, P., Chien, M., Chai, S., Hitotsumatsu, O., et al. (2004). The ubiquitin-modifying enzyme A20 is required for termination of Toll-like receptor responses. Nat. Immunol. *5*, 1052–1060.

Brint, E.K., Xu, D., Liu, H., Dunne, A., McKenzie, A.N., O'Neill, L.A., and Liew, F.Y. (2004). ST2 is an inhibitor of interleukin 1 receptor and Toll-like receptor 4 signaling and maintains endotoxin tolerance. Nat. Immunol. *5*, 373–379.

Burns, K., Janssens, S., Brissoni, B., Olivos, N., Beyaert, R., and Tschopp, J. (2003). Inhibition of interleukin 1 receptor/Toll-like receptor signaling through the alternatively spliced, short form of MyD88 is due to its failure to recruit IRAK-4. J. Exp. Med. *197*, 263–268.

Chuang, T.H., and Ulevitch, R.J. (2004). Triad3A, an E3 ubiquitin-protein ligase regulating Toll-like receptors. Nat. Immunol. *5*, 495–502.

Diehl, G.E., Yue, H.H., Hsieh, K., Kuang, A.A., Ho, M., Morici, L.A., Lenz, L.L., Cado, D., Riley, L.W., and Winoto, A. (2004). TRAIL-R as a negative regulator of innate immune cell responses. Immunity *21*, 877–889.

Divanovic, S., Trompette, A., Atabani, S.F., Madan, R., Golenbock, D.T., Visintin, A., Finberg, R.W., Tarakhovsky, A., Vogel, S.N., Belkaid, Y., et al. (2005). Negative regulation of Toll-like receptor 4 signaling by the Toll-like receptor homolog RP105. Nat. Immunol. *6*, 571–578.

Eriksson, U., Ricci, R., Hunziker, L., Kurrer, M.O., Oudit, G.Y., Watts, T.H., Sonderegger, I., Bachmaier, K., Kopf, M., and Penninger, J.M.

(2003). Dendritic cell-induced autoimmune heart failure requires cooperation between adaptive and innate immunity. Nat. Med. *9*, 1484–1490.

Fiorini, E., Schmitz, I., Marissen, W.E., Osborn, S.L., Touma, M., Sasada, T., Reche, P.A., Tibaldi, E.V., Hussey, R.E., Kruisbeek, A.M., et al. (2002). Peptide-induced negative selection of thymocytes activates transcription of an NF-kappa B inhibitor. Mol. Cell *9*, 637–648.

Fukao, T., Tanabe, M., Terauchi, Y., Ota, T., Matsuda, S., Asano, T., Kadowaki, T., Takeuchi, T., and Koyasu, S. (2002). PI3K-mediated negative feedback regulation of IL-12 production in DCs. Nat. Immunol. *3*, 875–881.

Hirotani, T., Lee, P.Y., Kuwata, H., Yamamoto, M., Matsumoto, M., Kawase, I., Akira, S., and Takeda, K. (2005). The nuclear IkappaB protein IkappaBNS selectively inhibits lipopolysaccharide-induced IL-6 production in macrophages of the colonic lamina propria. J. Immunol. *174*, 3650–3657.

Honda, K., Yanai, H., Negishi, H., Asagiri, M., Sato, M., Mizutani, T., Shimada, N., Ohba, Y., Takaoka, A., Yoshida, N., and Taniguchi, T. (2005). IRF-7 is the master regulator of type-I interferon-dependent immune responses. Nature *434*, 772–777.

Iwasaki, A., and Medzhitov, R. (2004). Toll-like receptor control of the adaptive immune responses. Nat. Immunol. *5*, 987–995.

Kawai, T., Adachi, O., Ogawa, T., Takeda, K., and Akira, S. (1999). Unresponsiveness of MyD88-deficient mice to endotoxin. Immunity *11*, 115–122.

Kinjyo, I., Hanada, T., Inagaki-Ohara, K., Mori, H., Aki, D., Ohishi, M., Yoshida, H., Kubo, M., and Yoshimura, A. (2002). SOCS1/JAB is a negative regulator of LPS-induced macrophage activation. Immunity *17*, 583–591.

Kisielow, P., Bluthmann, H., Staerz, U.D., Steinmetz, M., and von Boehmer, H. (1988). Tolerance in T-cell-receptor transgenic mice involves deletion of nonmature CD4+8+ thymocytes. Nature *333*, 742–746.

Kitajima, S., Takuma, S., and Morimoto, M. (1999). Changes in colonic mucosal permeability in mouse colitis induced with dextran sulfate sodium. Exp. Anim. *48*, 137–143.

Kobayashi, K., Hernandez, L.D., Galan, J.E., Janeway, C.A., Jr., Medzhitov, R., and Flavell, R.A. (2002). IRAK-M is a negative regulator of Toll-like receptor signaling. Cell *110*, 191–202.

Kobayashi, M., Kweon, M.N., Kuwata, H., Schreiber, R.D., Kiyono, H., Takeda, K., and Akira, S. (2003). Toll-like receptor-dependent production of IL-12p40 causes chronic enterocolitis in myeloid cell-specific Stat3-deficient mice. J. Clin. Invest. *111*, 1297–1308.

Kuhn, R., Lohler, J., Rennick, D., Rajewsky, K., and Muller, W. (1993). Interleukin-10-deficient mice develop chronic enterocolitis. Cell *75*, 263–274.

Kuwata, H., Watanabe, Y., Miyoshi, H., Yamamoto, M., Kaisho, T., Takeda, K., and Akira, S. (2003). IL-10-inducible Bcl-3 negatively regulates LPS-induced TNF-alpha production in macrophages. Blood *102*, 4123–4129.

Lang, K.S., Recher, M., Junt, T., Navarini, A.A., Harris, N.L., Freigang, S., Odermatt, B., Conrad, C., Ittner, L.M., Bauer, S., et al. (2005). Toll-like receptor engagement converts T-cell autoreactivity into overt autoimmune disease. Nat. Med. *11*, 138–145.

Lawrence, T., Bebien, M., Liu, G.Y., Nizet, V., and Karin, M. (2005). IKKalpha limits macrophage NF-kappaB activation and contributes to the resolution of inflammation. Nature *434*, 1138–1143.

Leadbetter, E.A., Rifkin, I.R., Hohlbaum, A.M., Beaudette, B.C., Shlomchik, M.J., and Marshak-Rothstein, A. (2002). Chromatin-IgG complexes activate B cells by dual engagement of IgM and Toll-like receptors. Nature *416*, 603–607.

Li, Q., Lu, Q., Bottero, V., Estepa, G., Morrison, L., Mercurio, F., and Verma, I.M. (2005). Enhanced NF-(kappa)B activation and cellular function in macrophages lacking I(kappa)B kinase 1 (IKK1). Proc. Natl. Acad. Sci. USA *102*, 12425–12430.

Liew, F.Y., Xu, D., Brint, E.K., and O'Neill, L.A. (2005). Negative regulation of Toll-like receptor-mediated immune responses. Nat. Rev. Immunol. *5*, 446–458.

Michelsen, K.S., Wong, M.H., Shah, P.K., Zhang, W., Yano, J., Doherty, T.M., Akira, S., Rajavashisth, T.B., and Arditi, M. (2004). Lack of Toll-like receptor 4 or myeloid differentiation factor 88 reduces atherosclerosis and alters plaque phenotype in mice deficient in apolipoprotein E. Proc. Natl. Acad. Sci. USA *101*, 10679–10684.

Moore, K.W., de Waal Malefyt, R., Coffman, R.L., and O'Garra, A. (2001). Interleukin-10 and the interleukin-10 receptor. Annu. Rev. Immunol. *19*, 683–765.

Motoyama, M., Yamazaki, S., Eto-Kimura, A., Takeshige, K., and Muta, T. (2005). Positive and negative regulation of nuclear factor-kappaB-mediated transcription by IkappaB-zeta, an inducible nuclear protein. J. Biol. Chem. *280*, 7444–7451.

Nakagawa, R., Naka, T., Tsutsui, H., Fujimoto, M., Kimura, A., Abe, T., Seki, E., Sato, S., Takeuchi, O., Takeda, K., et al. (2002). SOCS-1 participates in negative regulation of LPS responses. Immunity *17*, 677–687.

Natoli, G., Saccani, S., Bosisio, D., and Marazzi, I. (2005). Interactions of NF-kappaB with chromatin: the art of being at the right place at the right time. Nat. Immunol. *6*, 439–445.

Pasare, C., and Medzhitov, R. (2004). Toll-dependent control mechanisms of CD4 T cell activation. Immunity *21*, 733–741.

Saccani, S., Marazzi, I., Beg, A.A., and Natoli, G. (2004). Degradation of promoter-bound p65/RelA is essential for the prompt termination of the nuclear factor kappaB response. J. Exp. Med. *200*, 107–113.

Sakaguchi, S., Negishi, H., Asagiri, M., Nakajima, C., Mizutani, T., Takaoka, A., Honda, K., and Taniguchi, T. (2003). Essential role of IRF-3 in lipopolysaccharide-induced interferon-beta gene expression and endotoxin shock. Biochem. Biophys. Res. Commun. *306*, 860–866.

Strober, W., Fuss, I.J., and Blumberg, R.S. (2002). The immunology of mucosal models of inflammation. Annu. Rev. Immunol. *20*, 495–549.

Takaoka, A., Yanai, H., Kondo, S., Duncan, G., Negishi, H., Mizutani, T., Kano, S., Honda, K., Ohba, Y., Mak, T.W., and Taniguchi, T. (2005). Integral role of IRF-5 in the gene induction programme activated by Toll-like receptors. Nature *434*, 243–249.

Takeda, K., Clausen, B.E., Kaisho, T., Tsujimura, T., Terada, N., Forster, I., and Akira, S. (1999). Enhanced Th1 activity and development of chronic enterocolitis in mice devoid of Stat3 in macrophages and neutrophils. Immunity *10*, 39–49.

Wald, D., Qin, J., Zhao, Z., Qian, Y., Naramura, M., Tian, L., Towne, J., Sims, J.E., Stark, G.R., and Li, X. (2003). SIGIRR, a negative regulator of Toll-like receptor-interleukin 1 receptor signaling. Nat. Immunol. *4*, 920–927.

Wessells, J., Baer, M., Young, H.A., Claudio, E., Brown, K., Siebenlist, U., and Johnson, P.F. (2004). BCL-3 and NF-kappaB p50 attenuate lipopolysaccharide-induced inflammatory responses in macrophages. J. Biol. Chem. *279*, 49995–50003.

Yamamoto, M., Sato, S., Hemmi, H., Hoshino, K., Kaisho, T., Sanjo, H., Takeuchi, O., Sugiyama, M., Okabe, M., Takeda, K., and Akira, S. (2003). Role of adaptor TRIF in the MyD88-independent toll-like receptor signaling pathway. Science *301*, 640–643.

Yamamoto, M., Yamazaki, S., Uematsu, S., Sato, S., Hemmi, H., Hoshino, K., Kaisho, T., Kuwata, H., Takeuchi, O., Takeshige, K., et al. (2004). Regulation of Toll/IL-1-receptor-mediated gene expression by the inducible nuclear protein IkappaBzeta. Nature *430*, 218–222.

Mucosal Vaccine Targeting Improves Onset of Mucosal and Systemic Immunity to Botulinum Neurotoxin A[1]

Massimo Maddaloni,* Herman F. Staats,† Dagmara Mierzejewska,‡ Teri Hoyt,* Amy Robinson,* Gayle Callis,* Shunji Kozaki,§ Hiroshi Kiyono,¶ Jerry R. McGhee,‖ Kohtaro Fujihashi,‖ and David W. Pascual[2]*

Absence of suitable mucosal adjuvants for humans prompted us to consider alternative vaccine designs for mucosal immunization. Because adenovirus is adept in binding to the respiratory epithelium, we tested the adenovirus 2 fiber protein (Ad2F) as a potential vaccine-targeting molecule to mediate vaccine uptake. The vaccine component (the host cell-binding domain to botulinum toxin (BoNT) serotype A) was genetically fused to Ad2F to enable epithelial binding. The binding domain for BoNT was selected because it lies within the immunodominant H chain as a β-trefoil (Hcβtre) structure; we hypothesize that induced neutralizing Abs should be protective. Mice were nasally immunized with the Hcβtre or Hcβtre-Ad2F, with or without cholera toxin (CT). Without CT, mice immunized with Hcβtre produced weak secretory IgA (sIgA) and plasma IgG Ab response. Hcβtre-Ad2F-immunized mice produced a sIgA response equivalent to mice coimmunized with CT. With CT, Hcβtre-Ad2F-immunized mice showed a more rapid onset of sIgA and plasma IgG Ab responses that were supported by a mixed Th1/Th2 cells, as opposed to mostly Th2 cells by Hcβtre-dosed mice. Mice immunized with adjuvanted Hcβtre-Ad2F or Hcβtre were protected against lethal BoNT serotype A challenge. Using a mouse neutralization assay, fecal Abs from Hcβtre-Ad2F or Hcβtre plus CT-dosed mice could confer protection. Parenteral immunization showed that the inclusion of Ad2F enhances anti-Hcβtre Ab titers even in the absence of adjuvant. This study shows that the Hcβtre structure can confer protective immunity and that use of Hcβtre-Ad2F gives more rapid and sustained mucosal and plasma Ab responses. *The Journal of Immunology,* **2006, 177: 5524–5532.**

Botulism occurs from the infection by *Clostridium botulinum* or by ingestion of its neurotoxin complex, resulting in flaccid paralysis (1, 2). Due to its potency, the illicit dissemination of botulinum neurotoxins (BoNT)[3] poses a major threat to the unprotected populace. Of the seven serotypes, serotypes A, B, and, to a minor extent, E are typically associated with botulism in humans, whereas serotype C mostly affects domestic animals (1, 2). The toxins are each naturally synthesized as a single 150-kDa polypeptide, requiring posttranslational proteolysis to yield a ~50-kDa fragment or L chain, containing the catalytic activity, and a 100-kDa component or H chain (~100 kDa), containing the translocation domain in the N terminus and the cell-binding domain in the C terminus (Hc). Upon binding to the target cell, the translocation domain in the N terminus translocates the L chain to the cytosol, and the L chain endopeptidase activity inactivates a group of proteins (termed SNARE proteins) required for release of acetylcholine at the neuromuscular junction resulting in flaccid paralysis (3–6).

The current vaccine is a pentavalent one with as little at 10% of the toxoid preparation representing neurotoxoid (7), suggesting that much of the immune response induced by the vaccine is directed against vaccine components that will not contribute to protection against BoNT lethal challenge. Because formalin is used to inactivate BoNT to produce the toxoids for vaccine formulation, such chemical modification of the toxins results in a considerably altered tertiary structure (8) needed to elicit neutralizing Abs (9–11). Thus, better formulations are needed. To this end, structural analysis of the catalytic and binding sites of *C. botulinum* BoNT serotype B reveals that the Hc is structurally subdivided into a N-terminal subdomain, forming a jelly-roll motif, and a C-terminal subdomain, forming β-trefoil structure (5). We hypothesize that this β-trefoil structure contains the important neutralizing epitopes. In fact, in a previous study, neutralizing Abs against Hc BoNT serotype A (BoNT/A) exhibited two major protective epitopes, BoNT/$A_{455-661}$ and BoNT/$A_{1150-1289}$, which conferred ~75% protection, and one minor protective epitope, BoNT/$A_{780-939}$, which conferred 28% protection (9). The neutralizing epitope BoNT/$A_{1150-1289}$ conferred 75% protection and spanned about two-thirds of the β-trefoil region. Taken together, these results hint that the intact β-trefoil structure would be a potential candidate for an optimized vaccine.

Replication-deficient adenovirus vectors (12) and other viruses (13) have been experimentally used to correct genetic deficiencies, but these viral vectors have remained, in large part, immunogenic.

*Veterinary Molecular Biology, Montana State University, Bozeman, MT 59717; †Department of Pathology, Duke University Medical Center, Durham, NC 27710; ‡Department of Food Chemistry, Institute of Food Research, Polish Academy of Science, Olsztyn, Poland; §Laboratory of Veterinary Epidemiology, Graduate School of Agriculture and Biological Sciences, Osaka Prefecture University, Sakai-shi, Osaka, Japan; ¶Department of Microbiology and Immunology, Division of Mucosal Immunology, Institute for Medical Sciences, University of Tokyo, Tokyo, Japan; and ‖Department of Microbiology and Department of Pediatric Dentistry, University of Alabama at Birmingham, Birmingham, AL 35294

Received for publication April 5, 2006. Accepted for publication July 21, 2006.

The costs of publication of this article were defrayed in part by the payment of page charges. This article must therefore be hereby marked *advertisement* in accordance with 18 U.S.C. Section 1734 solely to indicate this fact.

[1] This work was supported by Public Health Service Grants DE-13812, AI-56286, AI-18958, DE-12242, AI-43197, and DC-04976, and in part by Montana Agricultural Station and the U.S. Department of Agriculture Formula Funds. The Veterinary Molecular Biology flow cytometry facility was supported in part by the Center of Biomedical Research Excellence P20 RR-020185 from the National Institutes of Health/National Center for Research Resources.

[2] Address correspondence and reprint requests to Dr. David W. Pascual, Veterinary Molecular Biology, P.O. Box 173610, Montana State University, Bozeman, MT 59717-3610. E-mail address: dpascual@montana.edu

[3] Abbreviations used in this paper: BoNT, botulinum neurotoxin; Hcβtre, β-trefoil stucture of Hc for BoNT; Ad2F, adenovirus 2 fiber protein; AFC, Ab-forming cell; CFC, cytokine-forming cell; CM, complete medium; DAPI, 4′,6-diamidino-2-phenylindole; CT, cholera toxin; LN, lymph node. sIgA, secretory IgA.

0022-1767/06/$02.00

Despite this condition, adenovirus vectors retain the advantage of transfecting the airway epithelium (14, 15). However, examination of the adenovirus components shows that adenovirus adhesion is mediated by the interaction between its attachment or fiber protein and receptors on the cell surface (15). Study of adenovirus (16) and reovirus (17) attachment proteins reveals that they share a common feature in that they are homotrimeric to form a high-energy structure that springs open upon binding its cell receptor, thus triggering a series of events ultimately leading to the entry of the virus into the cell. Therefore, it may be possible that adenovirus 2 fiber protein (Ad2F) could potentially be used in lieu of the intact virus for mucosal targeting.

In an effort to improve the current BoNT vaccine, we adopted a two-prong approach to create a mucosal vaccine against BoNT/A. First, we questioned whether the β-trefoil structure, which is responsible for the cell-binding activity, would be sufficient to elicit neutralizing Abs because this structure is maintained in all serotypes, as well as in tetanus toxoid (18). Accordingly, our vaccine includes this β-trefoil structure. In addition, we hypothesize that a fusion protein between this β-trefoil structure from BoNT/A genetically fused to adhesin Ad2F attachment protein may enhance its immunogenicity and uptake by the common mucosal immune system.

In this study, we showed that the addition of the mucosal-targeting molecule, Ad2F, enhanced onset of plasma and mucosal Ab responses. Both vaccines (with and without Ad2F) conferred complete protection from systemic challenge with as much as 20,000 LD_{50} of the native BoNT/A. Upon evaluation of mucosal Abs to the immunodominant Hc as a β-trefoil (Hcβtre) structure, mice dosed with Hcβtre-Ad2F showed the best protection against the BoNT/A complex.

Materials and Methods

DNA manipulations

As shown by others (19), initial attempts to express the *C. botulinum* gene encoding the Hc BoNT/A gene in yeast failed to yield any protein. Consequently, a synthetic gene encoding for Hc BoNT/A amino acids R864 to L1295 (GenBank accession no. X52066) was designed for optimized expression in the yeast *Pichia pastoris*. Factors taken into account for the synthetic gene were yeast codon bias, the reduction of *C. botulinum* A/T content, and the necessity for not depleting any particular tRNA pools. The Hcβtre spans from position S1096 to L1295, as predicted by others (18). To clone the Hcβtre domain, we included 15 more amino acids upstream from the predicted Hcβtre beginning with K1076 to L1295 to facilitate proper folding of the relevant domain.

To clone the Hc BoNT/A gene into the expression vector, the synthetic gene encoding for Hc BoNT/A was amplified with primers containing *Eco*RI and *Sal*I restriction sites. Likewise, to clone the Hcβtre, this gene was amplified from the synthetic Hc BoNT/A using primers containing *Eco*RI and *Sal*I restriction sites. In both cases, the 5′ primers containing the *Eco*RI site also provided an ATG initiation codon embedded into an optimal Kozak's sequence. The PCR products were cloned into a pCRII TOPO cloning vector (Invitrogen Life Technologies), excised with *Eco*RI and *Sal*I, and cloned into the *P. pastoris* expression vector pPICZ B cut with *Eco*RI and *Xho*I. Such a vector is designed to provide a C-terminal histidine tag for subsequent protein purification. Adenovirus 2 fiber was amplified from genomic adenovirus 2 DNA (a gift from Dr. J. Chroboczek, European Molecular Biology Laboratory, Grenoble, France). Attempts to express the entire Ad2F were unsuccessful; thus, only the C-terminal region, starting from G378 to E582, was cloned. This region encompasses 1) a short stretch of amino acids rich in Gly (4 of 15), 2) the region containing the trimerizing domain, and 3) the region containing the globular domain, commonly referred to as the "knob," which is important for interacting with the coxsackievirus/adenovirus receptor on the cell surface (15). This region proved to be easily expressed in *P. pastoris*, even when fused to a variety of Ags or fluorescent proteins.

To make Hcβtre-Ad2F, Hcβtre was amplified with primers generating *Eco*RI and *Sal*I ends cloned and excised with *Eco*RI and *Sal*I. The mentioned region of Ad2F was amplified with primer generating *Sal*I and *Kpn*I ends, cloned, and excised with the corresponding enzymes. The vector pPICZ B was cut with *Eco*RI and *Kpn*I. Finally, Hcβtre-Ad2F was assembled via a tripartite ligation. Primers were designed to allow in-frame junction between the different components and the formation of a flexible joint between Hcβtre and the Ad2F. To make Red2-Ad2F, a similar strategy was adopted. Red2 gene was amplified with primers generating *Eco*RI and *Sal*I ends using pDsRed2 (BD Biosciences) as template, and fused to Ad2F as described. These constructs were transformed into *P. pastoris* by electroporation.

Protein expression, purification, and FACS analysis

Recombinant proteins were produced by shifting the carbon source from glycerol to methanol, as required with *P. pastoris*. Briefly, yeast cells were cultured in yeast nitrogen base-glycerol until OD 0.5–1.0. Cells were then harvested by centrifugation and resuspended in yeast nitrogen base-methanol for 36–48 h. Pelleted biomass was either used right away or stored at −80°C until needed. Cells were disrupted with a bead-beater in ice, and debris were cleared by centrifugation, followed by filtration through a 1.2-μm prefilter, then by filtration through a 0.45-μm filter under vacuum. The cleared supernatant was then applied to a Talon column (BD Biosciences), as per the manufacturer's instruction. Purified proteins were eluted, titrated, and loaded onto a 12% polyacrylamide gel. Recombinant Hcβtre proteins were analyzed by Coomassie-stained SDS-PAGE to assess the quality of the protein. The Red2-Ad2F was blotted and probed with a commercial rabbit anti-Red2 Abs (BD Biosciences).

Recombinant Ad2F-binding assay

The mouse fibroblast L929 cells, human HeLa cells, and human 293 cells (American Type Culture Collection) were grown according to the complete medium (CM): RPMI 1640 (Invitrogen Life Technologies), 10% FBS (Atlanta Biologicals), 10 mM HEPES buffer, 10 mM nonessential amino acids, 10 mM sodium pyruvate, 100 U/ml penicillin, and 100 μg/ml streptomycin. Confluent cells were detached by trypsinization, washed, and resuspended in FACS buffer (10 g/L of Dulbecco's PBS (Sigma-Aldrich) plus 2% FBS). Cells were incubated with 25 μg of Red2-Ad2F or Red2 (BD Clontech), and incubated at room temperature for 45 min. Cells were washed once with 3 ml of FACS buffer and resuspended in 200 μl of FACS buffer. Bound fluorescence was analyzed with a FACSCalibur (BD Biosciences).

Histological preparation

Mice were nasally dosed with 50 μg Red2-Ad2F, and after 90 min, mice were euthanized to harvest heads. The skin, tongue, and lower jaw were removed, and the remaining portion was embedded into OCT (Sakura Finetek) with the top of turbinates oriented in the bottom of plastic cryomold to avoid cutting teeth. Turbinates were then snap frozen at −80°C. Turbinate frozen sections were cut at −30°C in a Leica Cryocut 1850 (Leica Microsystems) using Instrumedics CryoJane Tape Transfer System and a D profile tungsten carbide cryostat knife (Delaware Diamond Knives) to retain the undecalcified bone with epithelial lining on a slide. Frozen sections were air dried 30 min, then cover-slipped unfixed using Prolong Gold ready-to-use Anti-Fade Reagent with 4′,6-diamidino-2-phenylindole (DAPI; Molecular Probes).

Immunizations

Specific pathogen-free BALB/c mice were obtained from the National Cancer Institute and maintained in the Animal Resources Center at Montana State University (Bozeman, MT). All mice were kept under pathogen-free conditions in individually ventilated cages under HEPA-filtered, barrier conditions and fed sterile food and water ad libitum. The mice were free of bacterial and viral pathogens, as determined by Ab screening and by histopathologic analysis of major organs and tissues. Mice between age 5 and 8 wk were immunized nasally with 50 μg of Hcβtre or Hcβtre-Ad2F plus 5 μg of cholera toxin (CT; List Biological Laboratories), and boosted with their respective vaccines on days 7 and 14 postprimary immunization with 2 μg of CT. For i.m. immunizations, BALB/c mice were immunized with equimolar amounts of Hcβtre Ag, which represented 50 μg of Hcβtre-Ad2F and 25 μg of Hcβtre on days 0, 7, and 14 with or without 1.0 μg of CT given at the anterior tibial tuberosity to ensure delivery into the muscle (20).

ELISA to detect BoNT/A β-trefoil Abs

Standard ELISA protocols were followed to quantitate the Abs induced to BoNT/A Hcβtre. Recombinant BoNT/A Hcβtre (5 μg/ml) was used to coat Maxisorp microtiter plates (Nunc) overnight at 4°C. Immune plasma, fecal extracts, or nasal washes from individual mice were evaluated for their